

Boosting CO₂-to-CO Evolution Using a Bimetallic Diketopyrrolopyrrole Tethered Rhenium Bipyridine Catalyst (Supporting Information)

Cody R. Carr[†], Josh D. B. Koenig[†], Michael J. Grant, Warren E. Piers*, and Gregory C. Welch*

Department of Chemistry, University of Calgary, 2500 University Drive N.W., Calgary,
Alberta, T2N 1N4, Canada.

[†] Authors contributed equally to this work

* Corresponding Authors:

Email: wpiers@ucalgary.ca & gregory.welch@ucalgary.ca

Phone Number: 1-403-210-7603

Keywords: CO₂ reduction; molecular catalysis; rhenium; bipyridine; Re(bpy);
diketopyrrolopyrrole; DPP

TABLE OF CONTENTS

1. Materials & Instrumentation	S2 – S4
2. Data Handling/Calculations	S5
3. Synthetic/Experimental Procedures	S6 – S12
4. ¹H & ¹³C NMR Spectroscopies	S13 – S21
5. MALDI-TOF MS & CHN Elemental Analysis	S22 – S25
6. UV-Vis-nIR / FTIR Spectroscopies	S26
7. Electrochemistry Under Argon and CO₂	S27 - S29
8. Electro-/Photocatalytic Experiments	S30 – S42
9. Comparison of Supported Lehn-Type Catalysts	S43
10. References	S43

1. Materials & Instrumentation

Materials: Colloidal imprinted carbon with 85 nm pore size (CIC-85) was prepared according to literature preparation.¹ Custom polymer PDPPPPTD (batch = BM-19B; MW = 28 kDa; $D_m = 3.9$) and starting material 2,5-dihydro-3,6-di-2-thienyl-pyrrolo[3,4-c]pyrrole-1,4-dione (DPP) were purchased from Brilliant Matters and used without further purification. Carbon paper AvCarb® MGL370 was purchased from Fuel Cells Stores. Glassy carbon plates was purchased from Tokai, Carbon, and glassy carbon small disk electrodes from CH Instruments, inc. All other reactants, reagents, and catalysts for synthesis were purchased from Millipore-Sigma or Fisher Scientific and used without further purification. All air-free reactions were carried out under an atmosphere of N₂ using standard glovebox or high vacuum line (Schlenk) techniques.

Elemental Analysis (CHN EA): Elemental analyses were performed by Johnson Li in the Chemical Instrumentation Facility at the UofC. A Perkin Elmer 2400 Series II CHN Elemental Analyzer was used to obtain CHN data, using ~1.5 mg of sample (with particle sizes ranging between 0.2 and 0.5 mm in diameter).

High-resolution MALDI-TOF (HR MALDI-TOF): High-resolution MALDI-TOF mass spectrometry measurements were performed courtesy of Johnson Li in the Chemical Instrumentation Facility at the University of Calgary (UofC). Sample solution (~1 µg/mL in CH₂Cl₂) was mixed with matrix trans-2-[3-(4-tert-Butylphenyl)-2-methyl-2-propenylidene] malononitrile (DCTB) solution (~5 mg/ml in methanol). All spectra were acquired using a Bruker Autoflex III Smartbeam MALDI-TOF, set to the positive reflective mode (Na:YAG 355 nm laser settings: laser offset = 62-69; laser frequency = 200 Hz; and number of shots = 300). The target used was Bruker MTP 384 ground steel plate target.

Nuclear Magnetic Resonance (NMR): All ¹H, ¹H-¹H COSY, and ¹³C NMR spectroscopy experiments were recorded using a Bruker Fourier 300 MHz, Avance III 400 MHz, or a Avance III 600 MHz spectrometer. All experiments were performed in either chloroform-d (CDCl₃) or tetrachloroethane-d₂ (TCE-d₂). Chemical shifts (referenced to residual solvent) were reported in parts per million (ppm). ¹H NMR spectra used for quantitation of liquid CO₂ reduction products were recorded on a Bruker AV-III 500 MHz NMR spectrometer at room temperature. The measurements were carried out in with a standardized DMF in C₆D₆ segregated from aqueous analyte solution by internal capillary. Chemical shifts were reported in parts per million (ppm) and were referenced to residual proteo-benzene resonances. The relaxation delay was set to 50 s and 8 scans were measured for each sample. Aliquots volumes of 1 mL post CPE solutions were analyzed for liquid products.

UV-Visible Spectroscopy (UV-Vis): Optical absorption measurements were performed using Agilent Technologies Cary 60 UV-Vis spectrometer at ambient conditions. All solution UV-Vis spectra were measured with a 2 mm quartz cuvette, using CHCl₃ or N,N-dimethylformamide (DMF) as solvent. Stock solutions (~1 mg/mL) of each compound were prepared, serially diluted to concentrations between 10⁻⁵-10⁻⁶ M, and then used to construct calibration curves for determining molar absorptivity.

Fourier Transform Infrared Spectroscopy (FTIR): All IR absorption measurements were performed using an Agilent Technologies Cary 630 FTIR spectrometer at room temperature. FTIR

spectra were measured from CHCl_3 or DMF solutions of the analyte, using either the dial-path module (pathlength = 100 microns) or the transmission module.

Non-Aqueous Electrochemistry: All non-aqueous electrochemical measurements were performed using a CH Instruments Inc. Model 620E Potentiostat. Cyclic voltammetry (CV) experiments were performed in anhydrous N,N-dimethylformamide (DMF) at scan rates between 50 and 25,000 mV s^{-1} with 0.1 M tetrabutylammonium hexafluorophosphate (TBAPF_6) supporting electrolyte. Solutions were sparged with dry gas for at least 5 minutes prior to measurements and potentials were referenced versus the ferrocene/ferrocenium redox couple ($\text{Fc}^{+/0}$). Constant potential electrolyses (CPEs) were performed with a customized two-compartment H-shaped cell (total volume of 44.1 mL). A glassy carbon plate (20 mm \times 8 mm \times 2 mm) was used as the working electrode, along with a Pt-mesh counter electrode, and a non-aqueous Ag/AgCl pseudo-reference electrode. The working compartment contained 0.5 mM catalyst, 0.1 M TBAPF_6 , and 3 M TFE (9 mL) and the counter compartment contained 0.1 M TBAPF_6 and 3 M TFE (9 mL). Ohmic drop was minimized by maintaining less than 1 cm between the working and reference electrode.

Aqueous Electrochemistry: All aqueous electrochemical measurements were performed using a CHI 660D Potentiostat. The aqueous cell was divided into two compartments (containing 20 mL of solution each) separated by ultra-fine glass frit. A glass side-arm equipped with Teflon screw stopper and Suba-septum was iteratively opened and closed to the working compartment at regular intervals during electrolysis to sample the headspace and purge the cell with a fresh atmosphere of CO_2 . Gaseous products contained in the headspace of the working electrode compartment were analysed by opening the working compartment to the glass side arm (total headspace volume is 48.0 ± 0.2 mL) at the Teflon screw stopper to allow for diffusion of gases into the side arm. The headspace was sampled through a Suba-septum at 30 minutes intervals using a gastight Vici pressure-Lok® syringe and analysed using GC to quantify gaseous products. After each injection the working compartment was purged for 5 min with a fresh atmosphere of CO_2 . The counter compartment equipped with an airflow adapter was opened to a stream of CO_2 to balance the pressure between the working and counter compartments of the cell during purge. One segment of time equates to 30 minutes of consecutive electrolysis. All CPE experiments in aqueous electrolyte were performed with a 600 seconds pre-electrolysis with the cell open to the flow of CO_2 .

Spectroelectrochemistry (SEC): All UV-vis SEC and FTIR SEC experiments were conducted using a LabOmak IR-SEC cell fitted with CaF_2 windows (pathlength = 0.2 mm), a Pt-mesh working electrode (WE), a Pt-wire counter electrode (CE), an Ag-wire pseudo-reference electrode (RE), and $\text{Fc}^{+/0}$ as an internal reference standard. The cell was filled with DMF solutions (~0.1 mL) containing 0.5 mM analyte and 0.1 M TBAPF_6 . Solutions were sparged with N_2 in a scintillation vial for 15 minutes prior to use. Blank DMF solutions containing 0.1 M TBAPF_6 were used to baseline correct spectra at each voltage step.

Electrochemical Impedance Spectroscopy (EIS): EIS was performed on a CHI 660D potentiostat at room temperature in a three-electrode configuration in aqueous 0.5 M KHCO_3 electrolyte solution saturated with CO_2 (pH = 7.4). The system was calibrated using a custom-built Randle cell to verify that the individual components of the cell could be accurately determined by circuit modeling. Working electrodes were either carbon paper or PDPPPTD on carbon paper, counter a Pt mesh, and reference Ag/AgCl electrode half-cell. All measurements were performed at 0.1 V vs RHE with an amplitude set to 10 mV and AC impedance recorded in the range from 0.01 to 100,000 Hz. Equivalent circuit modeling was performed using Pine Research

Instrumentation AfterMath software package version 1.6.10523. The circuit model was the best fit to empirical data with lowest χ^2 found using modified LM method and parametric weighting after a max of 500 iterations.

Gas chromatography (GC): GC headspace analysis (50 μL aliquots) was performed using an Agilent Technologies 7890B GC, equipped with a PoraPlot Q and PLOT molecular sieve (5 \AA) column (oven temperature 60 – 120 $^\circ\text{C}$) in series and a VICI pulsed discharge Helium ionization detector. The flow rate of the carrier gas (helium) was approximately 5 mL min^{-1} . The system was calibrated using a customized gas mixture, containing known concentrations of: H_2 , CO , CH_4 , ethylene, and ethane.

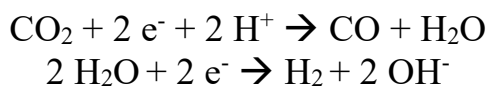
Scanning Electron Microscopy-Energy Dispersive X-Ray Spectroscopy (SEM-EDX): SEM-EDX images and spectra were recorded using a Zeiss Sigma VP instrument with an Inlens or SE2 detector at an accelerating voltage of 1-20 kV as indicated. EDX spectra were processed using the INCA software package.

Inductively Coupled Plasma Mass Spectrometry (ICP-MS): Measurements were performed using an Agilent ICP Triple Quadrupole Mass Spectrometer. The instrument was calibrated with a 10 mg L^{-1} Re in 2% HNO_3 certified reference standard, which was further diluted in 2% HNO_3 matrix to match with the collected KHCO_3 solution. Calibration was performed in a range from 0.0001 to 10 mg L^{-1} . Re content was measured at 182 amu using He as gas in the collision cell and Re at 217 amu using O_2 as gas in the collision cell. The 182 amu measurement has a reliable detection limit in the 30 ppt range, while the 217 amu measurement lies in the 100 ppt range. For both cases, calibrations curves showed linear behavior in the working range. The data was bracketed with calibration checks.

Contact Angle Wetting: Contact angle measurements were performed using an Ossila Contact Angle Goniometer. All samples were additionally dried in an oven set to 75 $^\circ\text{C}$ for 1 hr and then permitted to equilibrate to room temperature before the contact angle was measured by a single droplet containing 0.5 M KHCO_3 .

2. Data Handling/Calculations

- i) Faradaic efficiency (FE%) values were calculated from CPE at each 30-minute interval by considering the total charge (Q_t) counted by the potentiostat and charge consumed during CO_2 -to-CO or H_2O -to- H_2 conversion (Q_p) according to GC quantification and the stoichiometric half-reactions:



$$\begin{aligned}Q_p &= \text{mols product} \times n \times F \\ \text{FE\%} &= (Q_p/Q_t) \times 100\end{aligned}$$

Where: Q_p = conversion of charge into mols, $n = 2$ for both catalyzed reactions, F = Faradaic Constant (96485 C mol^{-1}), and FE\% = the ratio of Q_p by Q_t .

- ii) Current density (j) is reported as the measured total charge (Q_t) consumed during an interval of time (t) in seconds period per geometric area of carbon paper (A) in cm^2 :

$$j = Q_t/(t \times A)$$

- iii) Statistical analyses were performed using the conventional definition for average (\bar{x}), standard deviation (σ), and standard error ($\sigma_{\bar{x}}$) expressed as the error bars in the main text:

$$\begin{aligned}\bar{x} &= \frac{1}{N} \sum_{i=1}^N x_i \\ \sigma &= \pm \sqrt{\frac{\sum_{i=1}^N (x_i - \bar{x})^2}{N}} \\ \sigma_{\bar{x}} &= \frac{\sigma}{\sqrt{N}}\end{aligned}$$

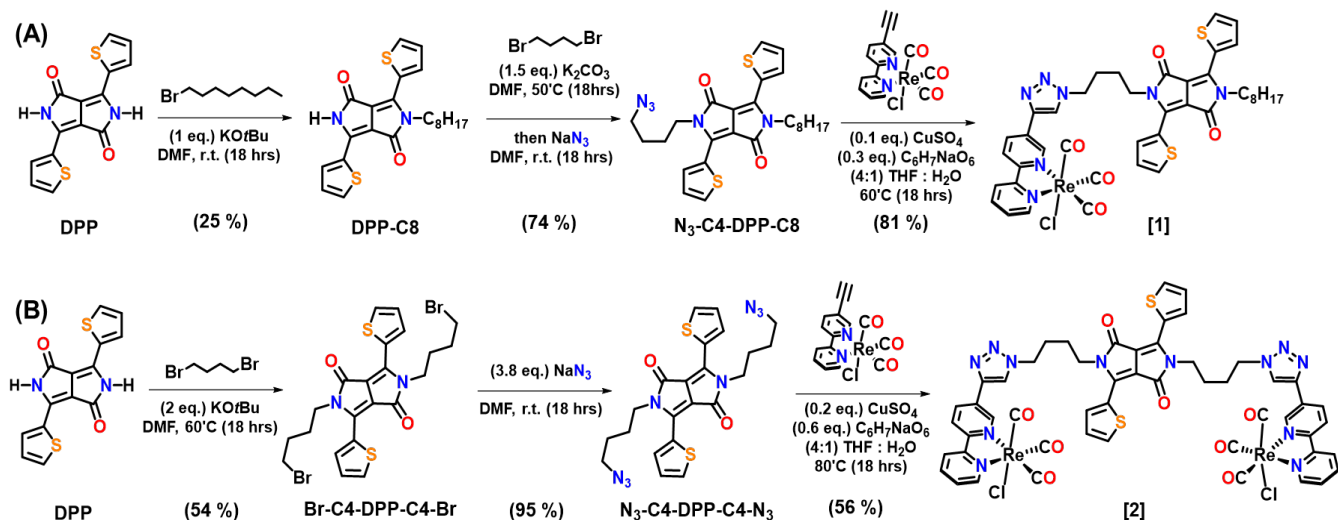
- iv) Quantitative $^1\text{H-NMR}$ was used to determine to formate concentration by referencing the integrated area of C-H proton in formate ($\delta = 8.46 \text{ ppm}$ in $\text{pH} = 7.4$) to the integrated area of the C-H proton in DMF ($\delta = 7.64 \text{ ppm}$ in benzene) via standardized solution of DMF in C_6D_6 :²

$$[\text{Formate}] = [\text{DMF}] \times (I_{\text{formate}}/I_{\text{DMF}})$$

Where: the concentration of formate and DMF are related by a factor ratio of the integrated peak areas (I_x).

3. Synthetic/Experimental Procedures

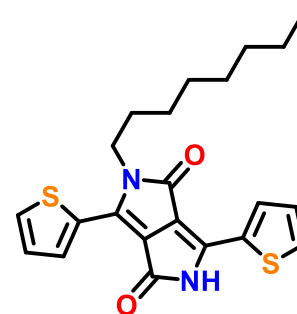
Scheme S1. Synthetic strategy for DPP tethered Re(bpy) catalysts **1** (A) and **2** (B).



Octyl Diketopyrrolopyrrole (DPP-C8)

Starting material, 2,5-dihydro-3,6-di-2-thienyl-pyrrolo[3,4-c]pyrrole-1,4-dione (DPP), was purchased from Brilliant Matters and used without further purification.

A 25 mL glass pressure vial was charged with DPP (600 mg, 2 mmol, 1 eq.) and potassium *tert*-butoxide (*t*BuOK; 225 mg, 2 mmol, 1 eq.) and dissolved in *N,N*-dimethylformamide (DMF; 20 mL). The vessel was sealed, sparged with N_2 for 15 mins, and then left to react for 1 hour at room temperature. Next, 1-bromooctane (0.35 mL, 2 mmol, 1 eq.) was slowly injected and then the reaction was left to stir for 17 hours. Solvent was subsequently removed under reduced pressure and then the crude material was re-dissolved in CH_2Cl_2 and poured over a silica plug. To purify the material, a (6:1) hexanes:acetone mixture was used to first elute the bis-alkylated material and then a (3:1) hexanes:acetone mixture was used to elute the desired mono-alkylated product. After solvent was removed, the isolated product was precipitated from H_2O and collected by vacuum filtration (206 mg, 0.50 mmol, 25 % yield).



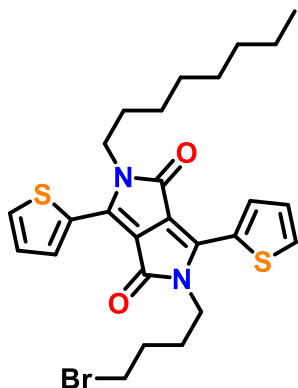
1H NMR (300 MHz, $CDCl_3$) δ 8.96 – 8.89 (m, 1H), 8.83 (s, 1H), 8.37 (d, J = 3.8 Hz, 1H), 7.69 (d, J = 4.9 Hz, 1H), 7.65 – 7.58 (m, 1H), 7.33 (t, J = 4.4 Hz, 1H), 7.25 (d, J = 4.4 Hz, 1H), 4.10 (t, J = 7.9 Hz, 2H), 1.76 (d, J = 8.3 Hz, 2H), 1.44 (m, 2H), 1.29 (m, 8H), 0.90 (t, J = 7.9 Hz, 3H).

^{13}C NMR (75 MHz, $CDCl_3$) δ 162.16, 161.33, 140.54, 136.26, 135.56, 131.99, 130.98, 130.82, 130.78, 129.78, 129.08, 128.63, 108.57, 108.10, 42.25, 31.78, 29.97, 29.71, 29.20, 26.88, 22.64, 14.10.

HRMS ($[M]^+$) calculated for $M = C_{22}H_{24}N_2O_2S_2$: 412.1274; detected $[M]^+$: 412.1281

1-bromobutyl-DPP-C8 (Br-C4-DPP-C8)

The alkylation procedure was modified from known literature.³



A 10 mL glass pressure vial was charged with DPP-C8 (206 mg, 0.5 mmol, 1 eq.) and potassium carbonate (K_2CO_3 ; 138 mg, 1 mmol, 2 eq.) and dissolved in DMF (5 mL). The vessel was sealed, sparged with N_2 for 15 mins, and then left to react for 1 hour at 60 °C. Next, 1,4-dibrombutane (0.30 mL, 2.5 mmol, 5 eq.) was slowly injected and then the reaction was left to stir for 17 hours. After solvent was removed under reduced pressure, the crude material was re-dissolved in CH_2Cl_2 and poured over a silica plug. To purify the material, a (6:1) hexanes:acetone mixture was used to elute the desired bis-alkylated product. Note, a (3:1) hexanes:acetone mixture can be used to recover unreacted mono-alkylated starting material. After solvent was removed, the isolated product was precipitated from H_2O and collected by vacuum filtration (205 mg, 0.38 mmol, 75 % yield).

1H NMR (300 MHz, $CDCl_3$) δ 9.04 – 8.84 (m, 2H), 7.67 (ddt, $J = 4.9, 2.4, 1.3$ Hz, 2H), 7.32 (ddd, $J = 5.1, 3.9, 1.2$ Hz, 2H), 4.16 (t, $J = 7.0$ Hz, 2H), 4.09 (t, $J = 7.9$ Hz, 2H), 3.47 (t, $J = 6.1$ Hz, 2H), 1.98 (q, $J = 7.7$ Hz, 4H), 1.76 (p, $J = 7.6$ Hz, 2H), 1.42 (m, 2H), 1.29 (m, 8H), 0.89 (t, $J = 6.3$ Hz, 3H).

^{13}C NMR (75 MHz, $CDCl_3$) δ 161.39, 161.36, 140.41, 139.59, 135.38, 135.30, 130.92, 130.68, 129.57, 128.75, 128.66, 108.00, 107.41, 42.27, 41.09, 32.95, 31.78, 29.98, 29.95, 29.20, 28.72, 26.88, 22.64, 22.62, 14.10.

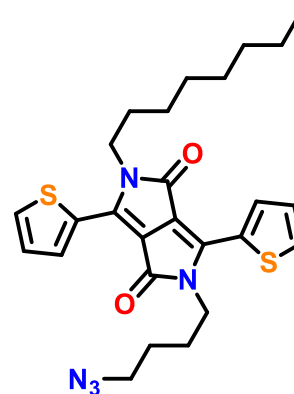
HRMS ($[M]^+$) calculated for $M = C_{26}H_{31}N_2O_2S_2Br$: 546.1005; detected $[M]^+$: 546.1029

1-azidobutyl-DPP-C8 (N_3 -C4-DPP-C8)

The azide substitution procedure was modified from known literature.⁴

Br-C4-DPP-C8 (205 mg, 0.38 mmol, 1 eq.) and sodium azide (NaN_3 ; 50 mg; 0.76 mmol; 2 eq.) were added to a 100 mL round bottom flask and dissolved in DMF (10 mL). The solution was sealed and left to stir overnight at room temperature. Upon reaction completion (as indicated by TLC), the mixture was poured into H_2O (75 mL) to induce precipitation. The resulting violet precipitate was collected by vacuum filtration (189 mg, 0.37 mmol, 98 % yield).

1H NMR (300 MHz, $CDCl_3$) δ 8.94 (td, $J = 3.7, 1.2$ Hz, 2H), 7.67 (ddd, $J = 5.1, 2.6, 1.1$ Hz, 2H), 7.31 (dd, $J = 5.0, 3.9$ Hz, 2H), 4.15 (t, $J = 7.4$ Hz, 2H), 4.12 – 4.03 (m, 2H), 3.36 (t, $J = 6.6$ Hz, 2H), 1.86 (qd, $J = 7.0, 3.7$ Hz, 2H), 1.74 (td, $J = 9.2, 4.3$ Hz, 4H), 1.42 (m, 2H), 1.29 (m, 8H), 0.93 – 0.84 (m, 3H).

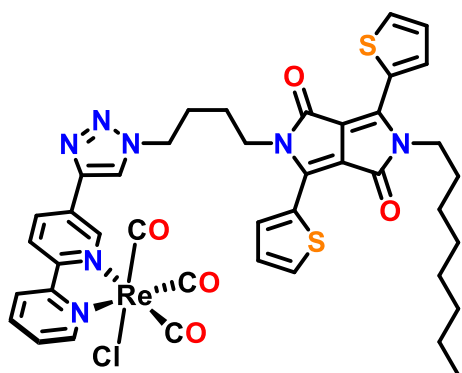


^{13}C NMR (75 MHz, CDCl_3) δ 161.39, 161.36, 140.43, 139.56, 135.47, 135.38, 135.33, 130.92, 130.65, 129.72, 129.57, 128.81, 128.76, 128.66, 107.99, 107.41, 51.01, 42.27, 41.40, 31.78, 29.95, 29.21, 29.19, 27.28, 26.88, 26.27, 22.63, 14.09.

HRMS ($[\text{M}]^+$) calculated for $\text{M} = \text{C}_{26}\text{H}_{31}\text{N}_5\text{O}_2\text{S}_2$: 509.1919; detected $[\text{M}]^+$: 509.1893

Re(bpy-C4-DPP-C8)(CO)₃Cl [1]

Starting material Re(5-ethynyl-2,2'-bipyridine)(CO)₃Cl was synthesized according to literature.⁵ Cooper catalyzed azide-alkyne cycloaddition was modified from literature procedure.⁴



Re(5-ethynyl-2,2'-bipyridine)(CO)₃Cl (48.6 mg, 0.10 mmol, 1 eq.) and N₃-C4-DPP-C8 (51 mg, 0.10 mmol, 1 eq.) were combined in a 10 mL glass pressure vial with CuSO₄ (1.6 mg, 0.010 mmol, 0.1 eq.) and sodium ascorbate (5.9 mg, 0.030 mmol, 0.3 eq.). The vial was sealed and then N₂-sparged for 30 minutes. A degassed mixture of (4:1) THF:H₂O (7.5 mL) was transferred into the vial using a Cannula line. The mixture was purged an additional 5 minutes, then placed into a 60 °C bath for 18 hours. Once TLC showed consumption of all starting material, solvent was removed under reduced pressure. The resulting crude solid(s) was re-dissolved in

CH₂Cl₂, adhered to silica, and then purified using a short silica plug. To purify the material, a (4:1) hexanes:acetone mixture was used to elute by-products and then a (4:3) hexanes:acetone mixture was used to elute the desired product. Solvent was removed under reduced pressure and the resulting pink-red solid was precipitated into a (19:1) MeOH:H₂O mixture and collected by vacuum filtration (81 mg, 0.08 mmol, 81 % yield).

^1H NMR (600 MHz, TCE-d₂) δ 8.70 (d, $J = 2.1$ Hz, 1H), 8.40 – 8.37 (m, 1H), 8.25 (dd, $J = 3.8$, 1.2 Hz, 1H), 8.23 (dd, $J = 3.9$, 1.2 Hz, 1H), 7.88 (dd, $J = 8.5$, 2.0 Hz, 1H), 7.58 (t, $J = 8.8$ Hz, 2H), 7.47 (dd, $J = 7.9$, 1.6 Hz, 1H), 7.45 (s, 1H), 7.07 (dd, $J = 5.0$, 1.2 Hz, 1H), 7.04 (dd, $J = 5.0$, 1.2 Hz, 1H), 6.94 – 6.90 (m, 1H), 6.66 (ddd, $J = 11.6$, 5.0, 3.9 Hz, 2H), 3.89 (t, $J = 7.1$ Hz, 2H), 3.52 (t, $J = 7.3$ Hz, 2H), 3.39 (t, $J = 8.0$ Hz, 2H), 1.46 (p, $J = 7.2$ Hz, 2H), 1.20 (q, $J = 7.6$ Hz, 2H), 1.12 – 1.06 (m, 2H), 0.77 (d, $J = 9.2$ Hz, 2H), 0.69 – 0.59 (m, 8H), 0.23 (t, $J = 6.8$ Hz, 3H).

^{13}C NMR (151 MHz, TCE-d₂) δ 196.78, 196.60, 188.81, 160.67, 160.66, 154.67, 153.63, 152.49, 149.09, 141.16, 140.08, 138.65, 138.61, 134.86, 134.79, 130.93, 130.48, 130.06, 129.02, 128.72, 128.35, 128.17, 126.51, 122.75, 122.60, 121.27, 107.48, 106.55, 49.64, 41.73, 40.28, 31.19, 29.81, 29.32, 28.64, 28.62, 26.84, 26.29, 22.10, 13.65.

HRMS ($[\text{M}-\text{Cl}]^+$) calculated for $\text{M} = \text{C}_{41}\text{H}_{39}\text{N}_7\text{O}_5\text{S}_2\text{ReCl}$: 958.1978; detected $[\text{M}-\text{Cl}]^+$: 958.1935

CHN theoretical (%) C: 49.46, H: 3.95, N: 9.85; found (%) C: 49.14, H: 4.03, N: 9.60

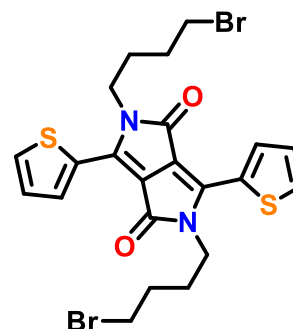
UV-vis λ ($\times 10^4 \text{ M}^{-1} \text{ cm}^{-1}$): 328 nm (3.2); 343 nm (3.0); 512 nm (2.0); 549 nm (2.4)

FTIR ν_{co} (cm^{-1}): 1894, 1916, and 2019 in DMF

Bis(1-bromobutyl)DPP (Br-C4-DPP-C4-Br)

DPP starting material was purchased from Brilliant Matters (see procedure for DPP-C8).

A 10 mL glass pressure vial was charged with DPP (150 mg, 0.50 mmol, 1 eq.) and *t*BuOK (125 mg, 1.1 mmol, 2.2 eq.) and then dissolved in DMF (6 mL). The vessel was sealed, sparged with N₂ for 15 mins, and then left to react for 1 hour at 60 °C. Next, 1,4-dibromobutane (0.30 mL, 2.5 mmol, 5 eq.) was slowly injected and then the reaction was left to stir for 17 hours. Solvent was subsequently removed under reduced pressure and then the crude material was re-dissolved in CH₂Cl₂ and poured over a silica plug. To purify the material, a (5:1) hexanes:acetone mixture was used to first elute the bis-alkylated product. Note, a (3:1) hexanes:acetone mixture can be used to elute the mono-alkylated product. After solvent was removed, the isolated product was precipitated from H₂O and collected by vacuum filtration (154 mg, 0.27 mmol, 54 % yield).



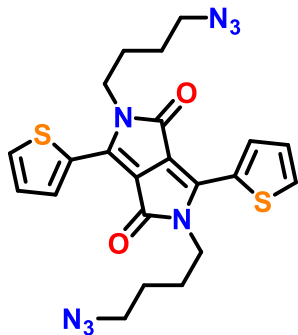
¹H NMR (400 MHz, CDCl₃) δ 8.93 (dd, *J* = 3.9, 1.2 Hz, 2H), 7.69 (dd, *J* = 5.0, 1.2 Hz, 2H), 7.33 (dd, *J* = 5.0, 3.9 Hz, 2H), 4.16 (t, *J* = 7.2 Hz, 4H), 3.47 (t, *J* = 6.3 Hz, 4H), 2.03 – 1.91 (m, 8H).

¹³C NMR (151 MHz, CDCl₃) δ 161.33, 139.93, 135.36, 130.86, 129.47, 128.75, 107.69, 41.09, 32.85, 29.95, 28.67.

HRMS ([M]⁺) calculated for M = C₂₂H₂₂N₂O₂S₂Br₂: 567.9489; detected [M]⁺: 567.9470

Bis(1-azidobutyl)DPP (N₃-C4-DPP-C4-N₃)

The azide substitution procedure was modified from known literature.⁴



Br-C4-DPP-C4-Br (154 mg, 0.27 mmol, 1 eq.) and sodium azide (NaN₃; 67 mg; 1.0 mmol; 3.7 eq.) were added to a 100 mL round bottom flask and dissolved in DMF (25 mL). The solution was sealed and left to stir overnight at room temperature. Upon reaction completion (as indicated by TLC), the mixture was poured into H₂O (75 mL) to induce precipitation. The resulting violet precipitate was collected by vacuum filtration (126 mg, 0.26 mmol, 96 % yield).

¹H NMR (400 MHz, CDCl₃) δ 8.94 (dd, *J* = 3.9, 1.2 Hz, 2H), 7.69 (dd, *J* = 5.0, 1.2 Hz, 2H), 7.33 (dd, *J* = 5.0, 3.9 Hz, 2H), 4.20 – 4.12 (m, 4H), 3.37 (t, *J* = 6.7 Hz, 4H), 1.92 – 1.83 (m, 4H), 1.74 (dtd, *J* = 15.1, 6.7, 1.0 Hz, 4H).

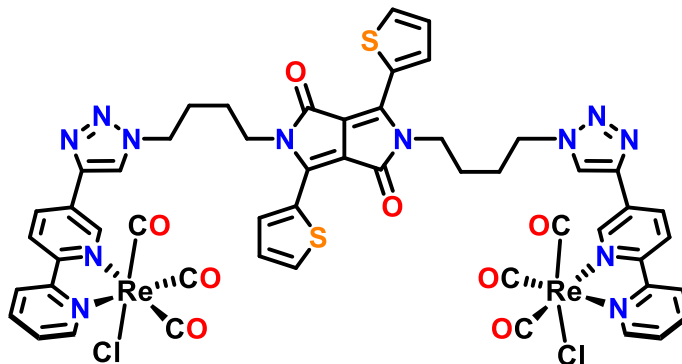
¹³C NMR (151 MHz, CDCl₃) δ 161.32, 139.89, 135.41, 130.85, 129.46, 128.75, 107.67, 50.97, 41.39, 27.23, 26.23.

HRMS ([M]⁺) calculated for M = C₂₂H₂₂N₈O₂S₂: 494.1307; detected [M]⁺: 494.1280

Cl(CO)₃Re(bpy-C4-DPP-C4-bpy)Re(CO)₃Cl [2]

Starting material Re(5-ethynyl-2,2'-bipyridine)(CO)₃Cl was synthesized according to literature.⁵ Cooper catalyzed azide-alkyne cycloaddition was modified from literature procedure.⁴

Re(5-ethynyl-2,2'-bipyridine)(CO)₃Cl (91.2 mg, 0.20 mmol, 1 eq.) and N₃-C4-DPP-C4-N₃ (50 mg, 0.10 mmol, 1 eq.) were combined in a 10 mL glass pressure vial with CuSO₄ (3.2 mg, 0.02 mmol, 0.2 eq.) and sodium ascorbate (11.6 mg, 0.06 mmol, 0.6 eq.). The vial was sealed and then N₂-sparged for 30 minutes. A degassed mixture of (4:1) THF:H₂O (10 mL) was transferred into the vial using a Cannula line. The mixture was purged an additional 5 minutes, then placed into a 70 °C bath for 18 hours. Once TLC showed consumption of all starting material, solvent was removed under reduced pressure. The resulting crude solid(s) was redissolved in CH₂Cl₂, adhered to silica, and then purified using a short silica plug. To purify the material, a (4:1) hexanes:acetone mixture was used to elute by-products and then a (4:3) hexanes:acetone mixture was used to elute the desired product. Solvent was removed under reduced pressure and the resulting pink-red solid was precipitated into a (19:1) MeOH:H₂O mixture and collected by vacuum filtration (82 mg, 0.056 mmol, 56 % yield).



¹H NMR (600 MHz, CD₂Cl₂) δ 8.69 (dd, *J* = 4.5, 2.0 Hz, 1H), 8.38 (d, *J* = 4.8 Hz, 1H), 8.22 (dd, *J* = 3.8, 1.2 Hz, 1H), 7.84 (ddd, *J* = 10.7, 8.3, 2.0 Hz, 1H), 7.61 – 7.57 (m, 2H), 7.46 (ddt, *J* = 7.9, 4.3, 1.9 Hz, 1H), 7.43 (d, *J* = 1.9 Hz, 1H), 7.06 (dd, *J* = 5.0, 1.2 Hz, 1H), 6.93 – 6.90 (m, 1H), 6.65 (ddd, *J* = 5.1, 3.8, 1.5 Hz, 1H), 3.89 (t, *J* = 7.1 Hz, 2H), 3.51 (q, *J* = 8.1 Hz, 2H), 1.51 – 1.39 (m, 2H), 1.25 – 1.15 (m, 2H).

¹³C NMR (151 MHz, CD₂Cl₂) δ 196.84, 196.64, 188.82, 160.69, 154.67, 153.62, 152.46, 149.04, 141.15, 139.27, 138.65, 134.96, 134.78, 130.89, 130.01, 128.65, 128.41, 126.51, 122.80, 122.67, 121.34, 107.04, 49.62, 40.29, 26.77, 26.15.

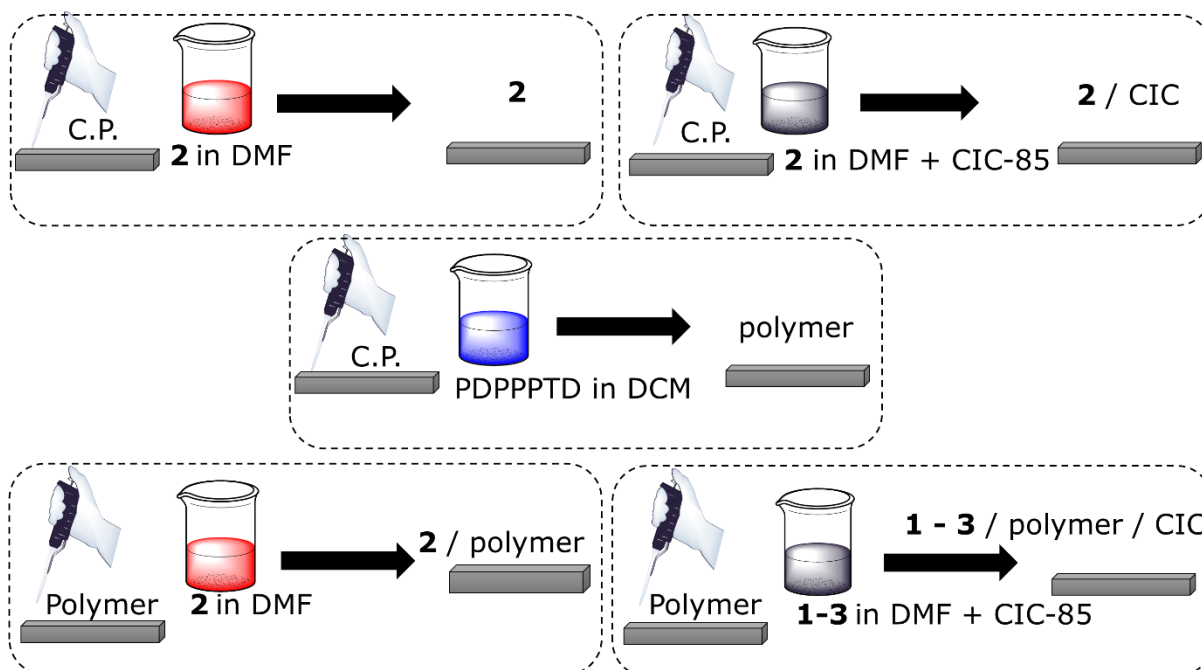
HRMS ([M-Cl]⁺) calculated for M = C₅₂H₃₈N₁₂O₈S₂Re₂Cl₂: 1466.09; detected [M-Cl]⁺: 1427.264

CHN theoretical (%) C: 42.59, H: 2.61, N: 11.46; found (%) C: 42.99, H: 2.81, N: 11.06

UV-vis λ (x 10⁴ M⁻¹ cm⁻¹): 328 nm (4.1); 343 nm (4.0); 512 nm (1.9); 549 nm (2.2)

FTIR ν_{co} (cm⁻¹): 1894, 1916, and 2019 in DMF

Scheme S2. Fabrication of electrodes by drop casting from solution; 10 mM solutions of **1 - 3** in DMF; 5 mg of CIC-85 in 1 mL of DMF; soluble fraction of PDPPPTD saturated in CH₂Cl₂ CP = carbon paper with geometric area of 6.2 cm², polymer = PDPPPTD on carbon paper.



Electrode preparation: Carbon paper was cut into 3.1×1 cm rectangle pieces using a razor blade and a straight edge. Carbon paper was modified for CO₂ electroreduction in aqueous 0.5 M KHCO₃ saturated with CO₂ (pH = 7.4) from drop casting solutions of catalysts **1-3**, PDPPPTD polymer, and CIC-85. Various solvents were trialed for the drop casting step and DMF was found to be the most effective. Error bars in reported data represent experiments performed with freshly prepared electrodes and all experiments performed a minimum of 3 times. Catalyst loading (Γ_{cat}) is $0.6 \mu\text{mol cm}^{-2}$ for all catalysts and CIC-85 is $\sim 0.3 \text{ mg cm}^{-2}$ with respect to the geometric area of carbon paper for all electrodes.

Catalyst 2 on glassy carbon: Thin films of **2** were formed by drop casting a 10 mM solution in DMF onto a 3×1 cm area of glassy carbon. The solution was evaporated over night (>16 hr), the film was then rinsed with milliQ water, and dried for additional 5 hrs at room temperature. PTFE tape was used as insulating material to cover exposed regions of the glassy carbon plate and reduce the catalyst film to an area of $\sim 0.5 \text{ cm}^2$.

Catalyst 2 on carbon paper: Solutions of 10 mM of catalysts **2** were prepared in 1 mL DMF by sonicating for 5 minutes. Using a micropipette, 200 μL of DMF solution was dropped evenly onto the surface of carbon paper and dried at room temperature for 5 hours. Notably, DMF solutions quickly absorb into the porous carbon paper. The carbon paper sample was then flipped after 5 hours to the “bare side” facing up, and another 200 μL aliquot was dropped and allowed to dry over night (>12 hours). The sample was finally rinsed with ≈ 1 mL milliQ water on each side and dried for 5 hours at room temperature before use.

Polymer PDPPPTD on carbon paper: Saturated solutions of PDPPPTD in DCM were prepared by adding 10 mg of PDPPPTD to 5 mL of DCM, sonicated for 1 hour, and rapidly stirred overnight whereupon the solution turned deep blue. The saturated solution was then filtered through a 0.2 μM syringe filter. Using a micropipette, 200 μL of the deep blue DCM solution was dropped onto carbon paper and dried for 1 hour at room temperature. The carbon paper sample was then flipped after 1 hours to the “bare side” facing up, and another 200 μL aliquot was dropped and dried again for 1 hour. This process was iterated for a total of $2 \times 200 \mu\text{L}$ per side and dried over night (>12 hours). The sample was finally rinsed with ≈ 1 mL milliQ water on each side and dried for 5 hours at room temperature before use.

CIC-85 on carbon paper: A suspension of CIC-85 in DMF was generated by adding 5 mg of CIC-85 to 1 mL of DMF and sonicating for 1 hour. Using a micropipette, 200 μL of suspension was dropped evenly onto the surface of carbon paper and dried at room temperature for 5 hours. The carbon paper sample was then flipped after 5 hours to the “bare side” facing up, and another 200 μL aliquot was dropped and allowed to dry over night (>12 hours). The sample was finally rinsed with ≈ 1 mL milliQ water on each side and dried for 5 hours at room temperature before use.

Catalyst 2 on PDPPPTD on carbon paper: Carbon paper was modified according to the preparation PDPPPTD on carbon paper (above). Following a drying period, catalyst **2** were dropped onto the modified surface according to the preparation catalyst **2** on carbon paper (above).

Catalyst 2 with CIC-85 on carbon paper: To solutions of 10 mM of catalysts **2**, 5 mg of CIC-85 were prepared in 1 mL DMF by sonicating for 1 hour. Using a micropipette, 200 μL of DMF solution/suspension was dropped evenly onto the surface of carbon paper and dried at room temperature for 5 hours. The carbon paper sample was then flipped after 5 hours to the “bare side” facing up, and another 200 μL aliquot was dropped and allowed to dry over night (>12 hours). The sample was finally rinsed with ≈ 1 mL milliQ water on each side and dried for 5 hours at room temperature before use.

Catalyst 1-3 with CIC-85 on PDPPPTD on carbon paper: Carbon paper was modified according to the preparation PDPPPTD on carbon paper (above). To solutions of 10 mM of catalysts **1-3**, 5 mg of CIC-85 were prepared in 1 mL DMF by sonicating for 1 hour. Using a micropipette, 200 μL of DMF solution/suspension was dropped evenly onto the surface of carbon paper and dried at room temperature for 5 hours. The carbon paper sample was then flipped after 5 hours to the “bare side” facing up, and another 200 μL aliquot was dropped and allowed to dry over night (>12 hours). The sample was finally rinsed with ≈ 1 mL milliQ water on each side and dried for 5 hours at room temperature before use. Electrodes made with **1** and **2** were desorbed into DMF following 3 hours of CPE. These solutions of **1** and **2** in DMF were then diluted by a factor of 1:100 for UV and IR spectral analysis.

4. ^1H & ^{13}C NMR Spectroscopies

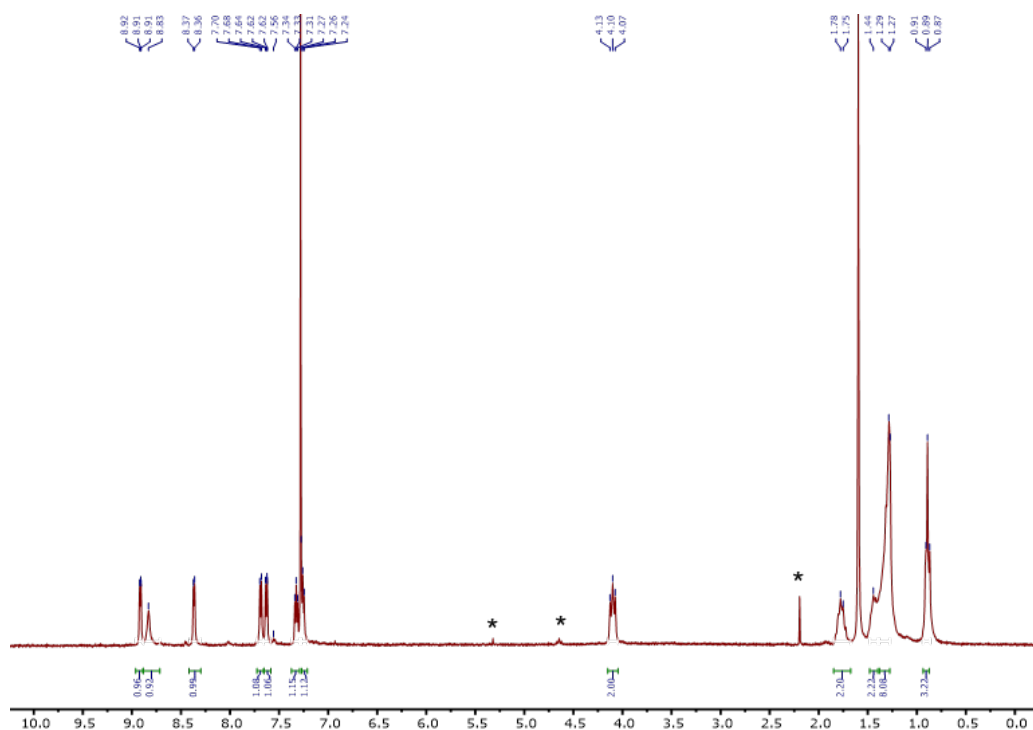


Figure S1. ^1H NMR spectrum of DPP-C8 (300 MHz, CDCl_3); *= solvent impurities⁶

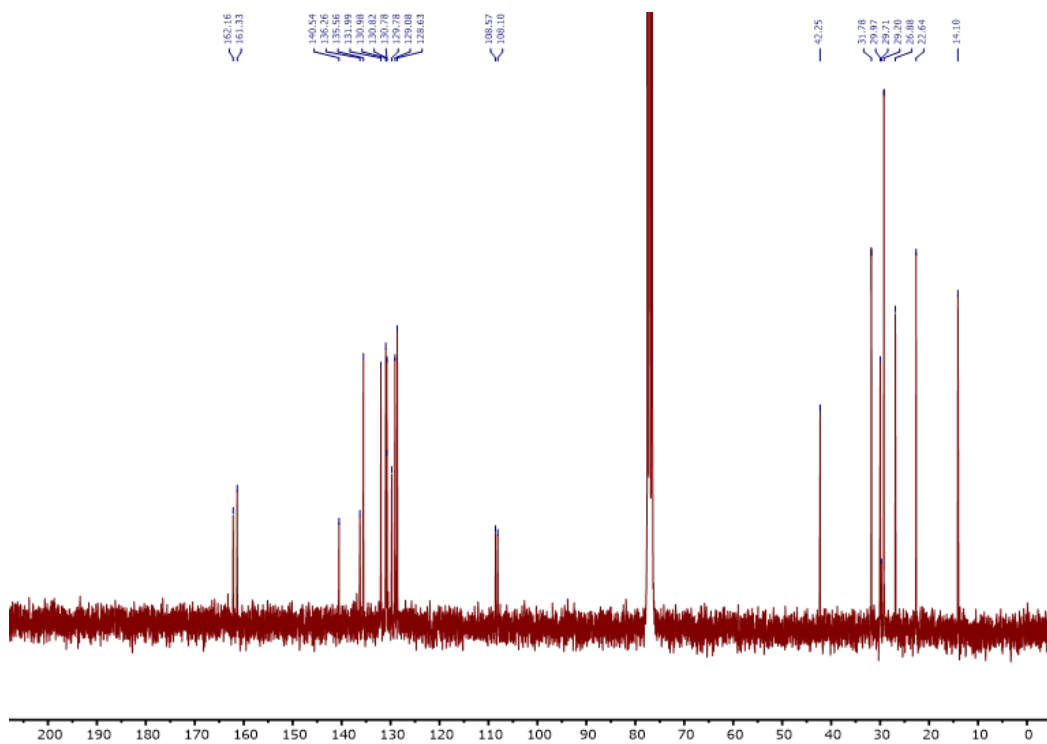


Figure S2. $^{13}\text{C}\{^1\text{H}\}$ NMR spectrum of DPP-C8 (75 MHz, CDCl_3)

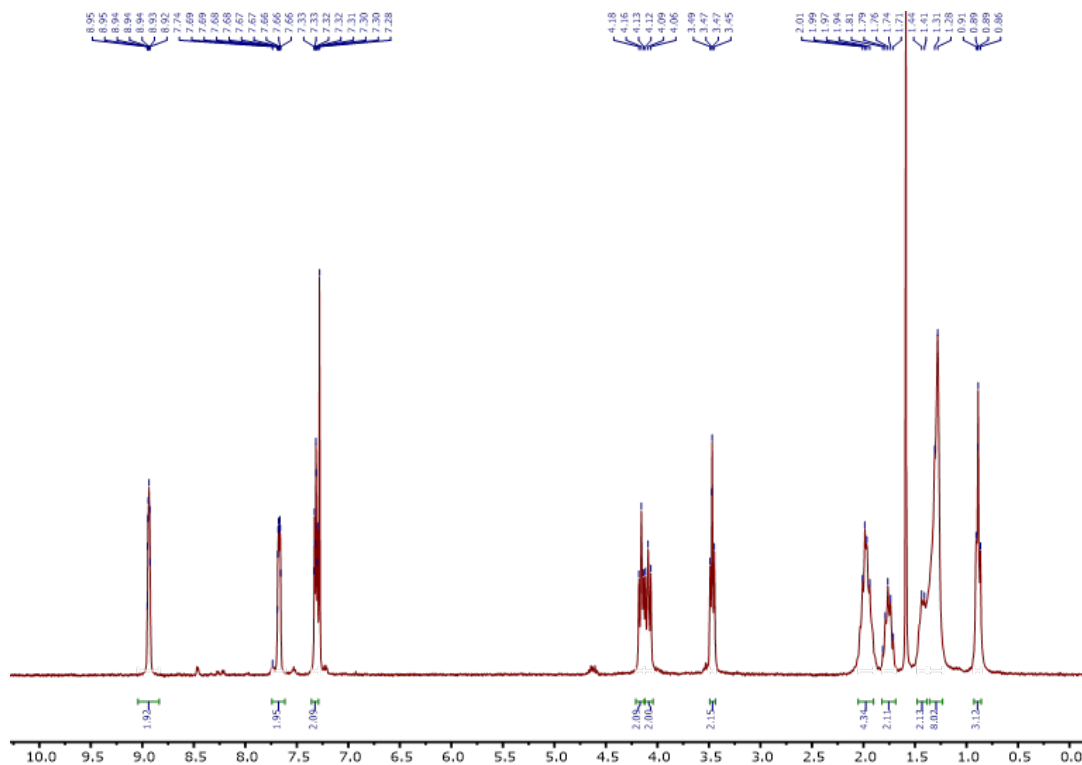


Figure S3. ^1H NMR spectrum of Br-C4-DPP-C8 (300 MHz, CDCl_3)

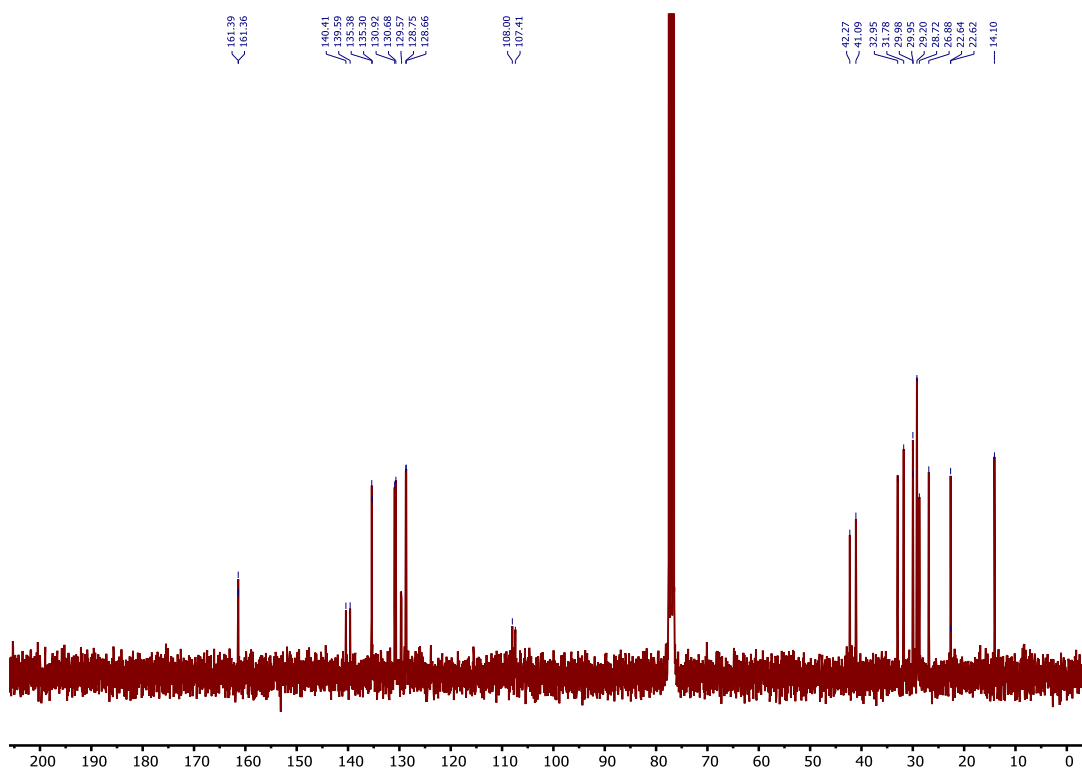


Figure S4. $^{13}\text{C}\{^1\text{H}\}$ NMR spectrum of Br-C4-DPP-C8 (75 MHz, CDCl_3)

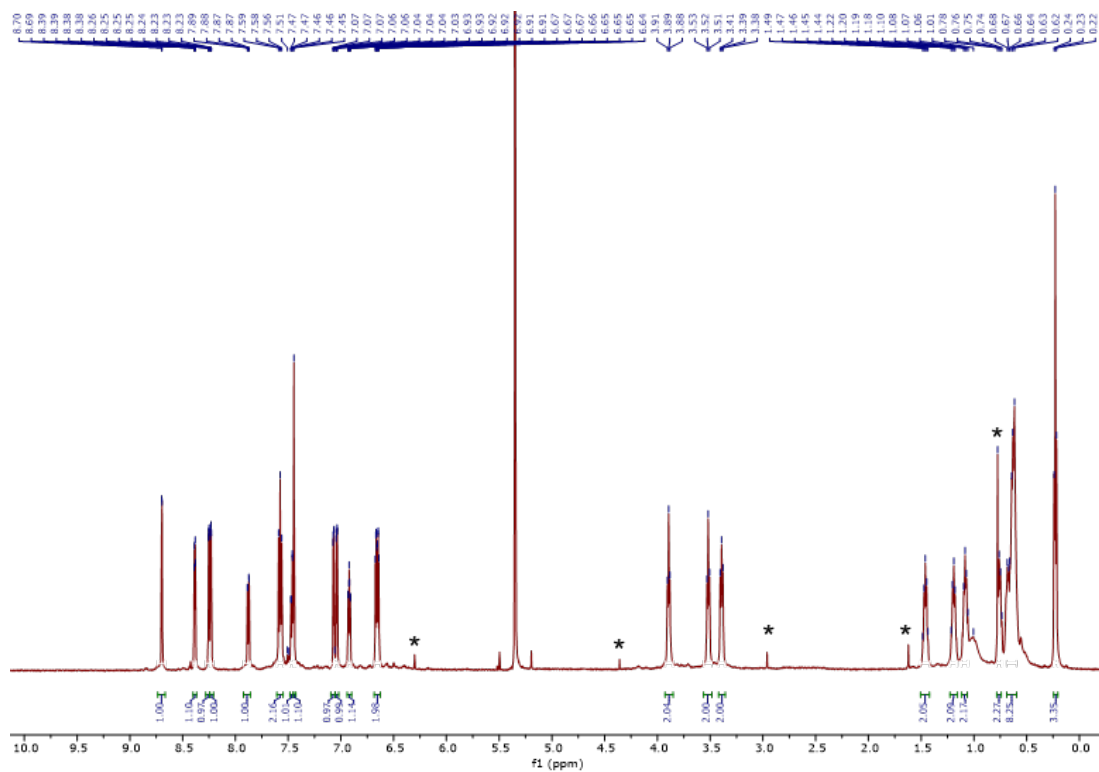


Figure S7. ^1H NMR spectrum of catalyst **1** (600 MHz, TCE-d_2); *= solvent impurities⁶

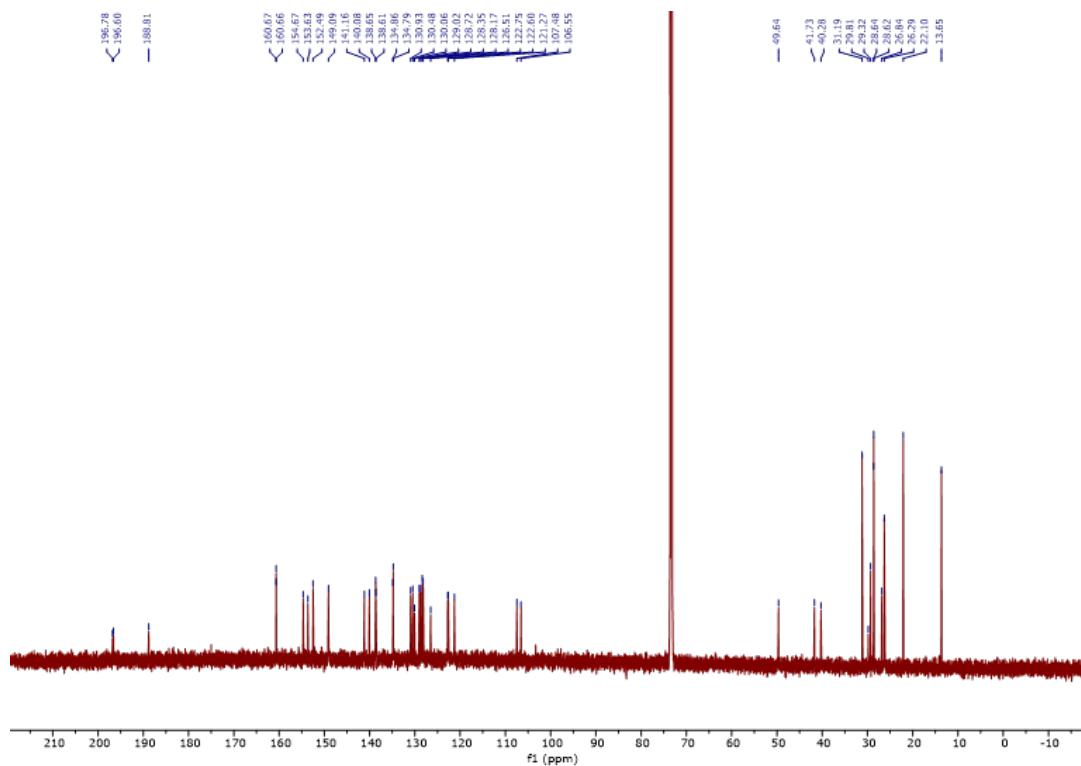


Figure S8. $^{13}\text{C}\{^1\text{H}\}$ NMR spectrum of catalyst **1** (151 MHz, TCE-d_2)

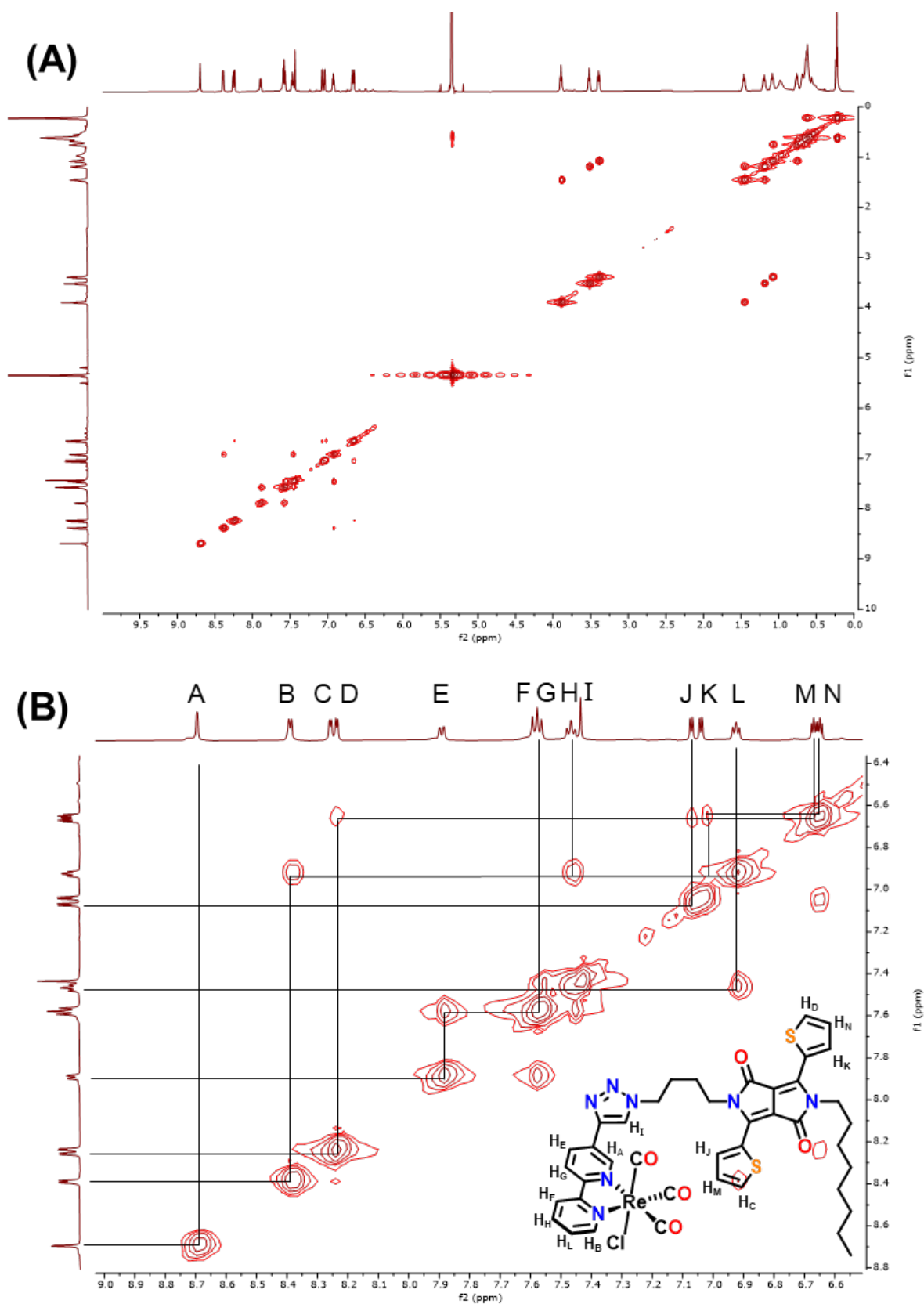


Figure S9. (A) Full ^1H - ^1H COSY spectrum with (B) enhanced view and assignment of aromatic protons for catalyst **1** (600 MHz, TCE- d_2)

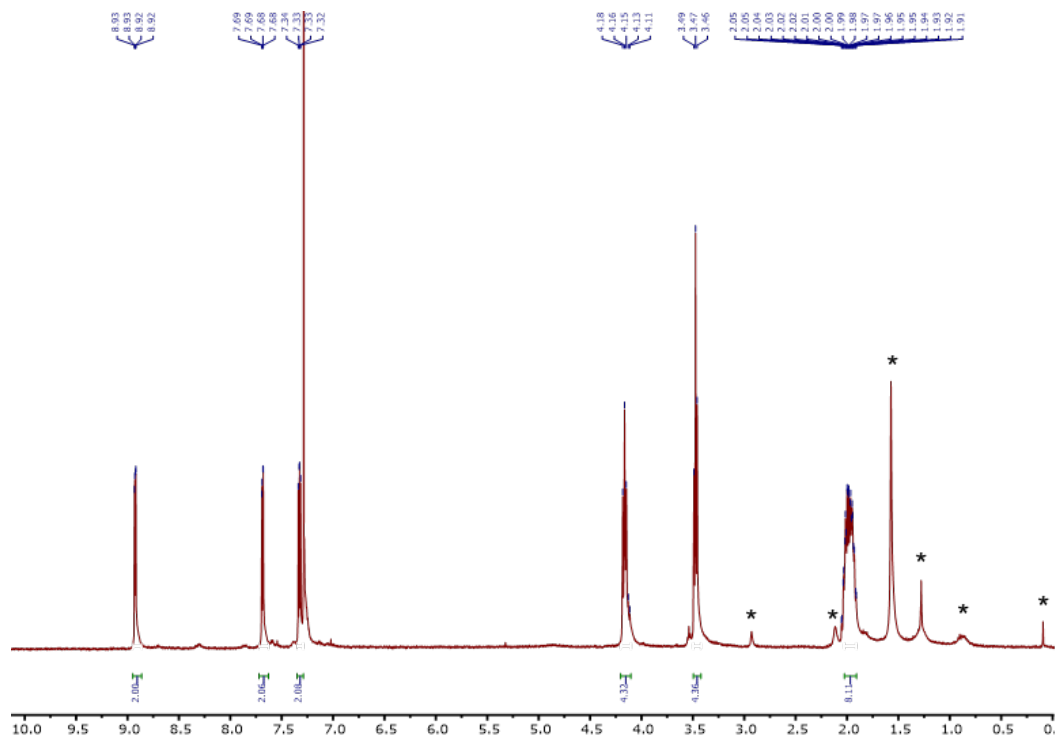


Figure S10. ^1H NMR spectrum of Br-C4-DPP-C4-Br (400 MHz, CDCl_3); *= solvent impurities⁶

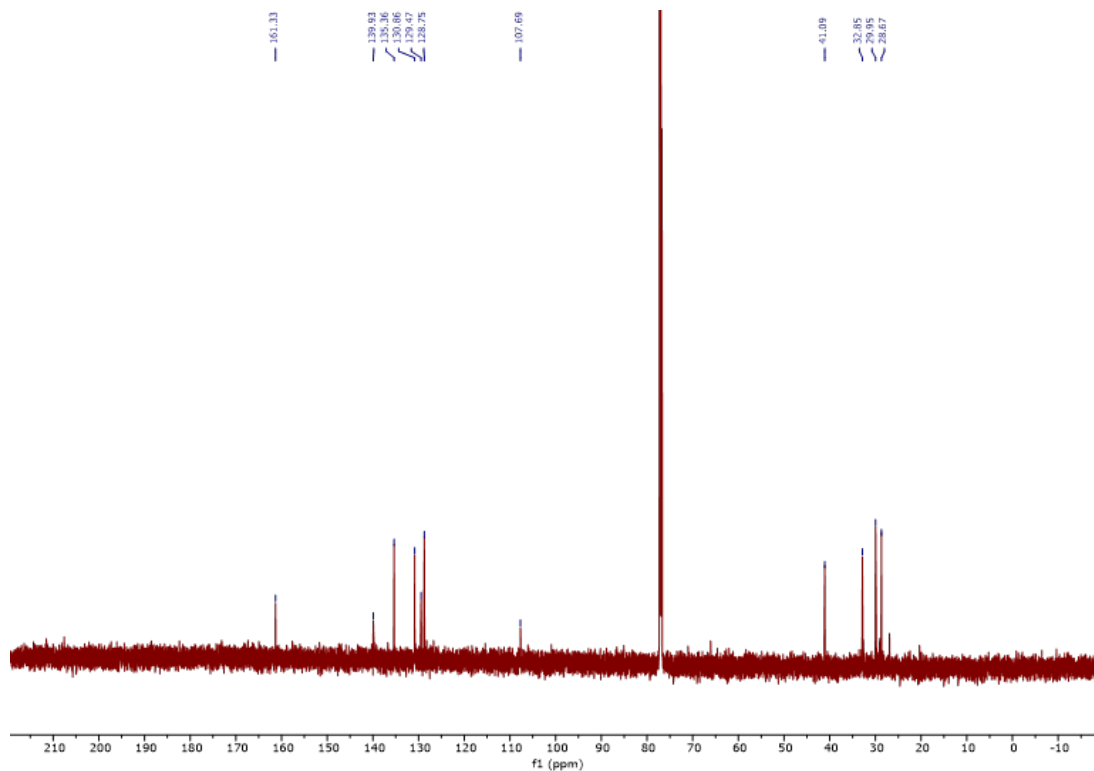


Figure S11. $^{13}\text{C}\{^1\text{H}\}$ NMR spectrum of Br-C4-DPP-C4-Br (151 MHz, CDCl_3)

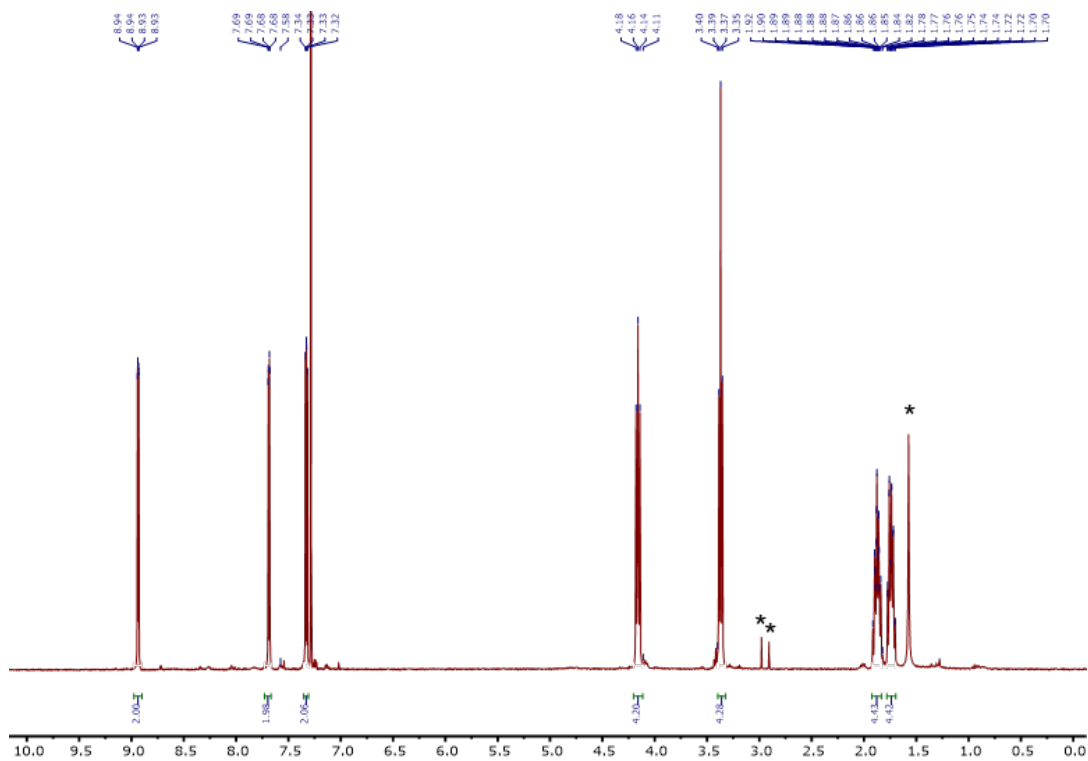


Figure S12. ^1H NMR spectrum of $\text{N}_3\text{-C}_4\text{-DPP-C}_4\text{-N}_3$ (300 MHz, CDCl_3); *= solvent impurities⁶

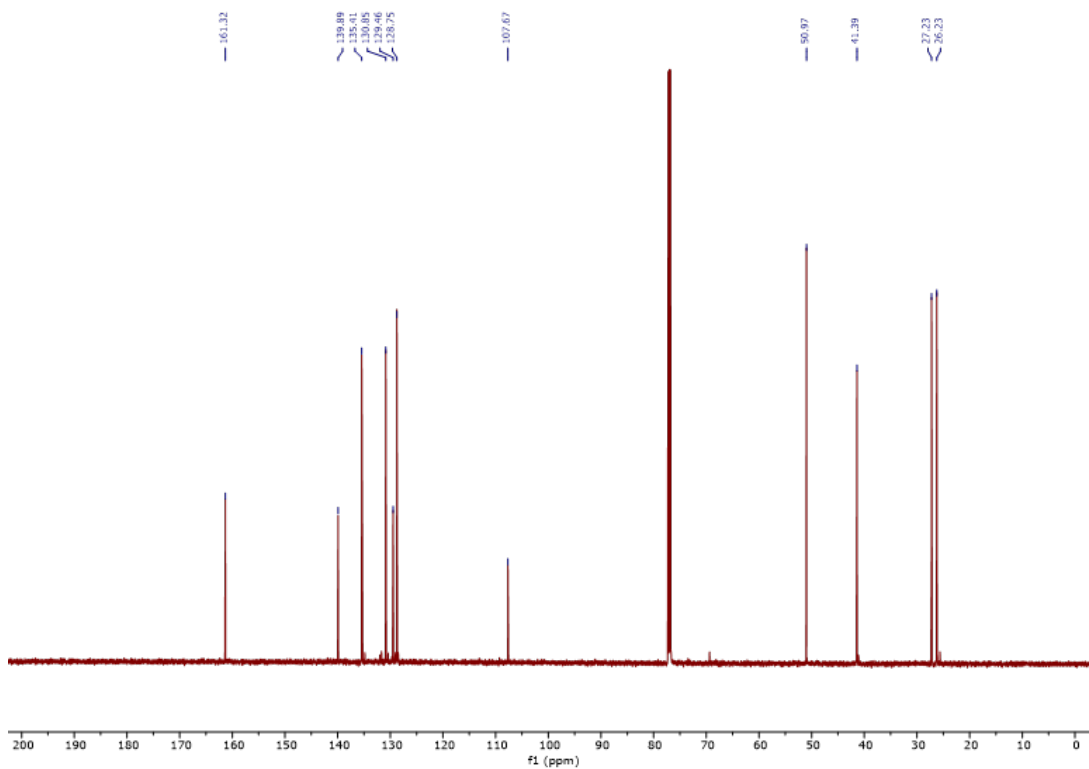


Figure S13. $^{13}\text{C}\{^1\text{H}\}$ NMR spectrum of $\text{N}_3\text{-C}_4\text{-DPP-C}_4\text{-N}_3$ (151 MHz, CDCl_3)

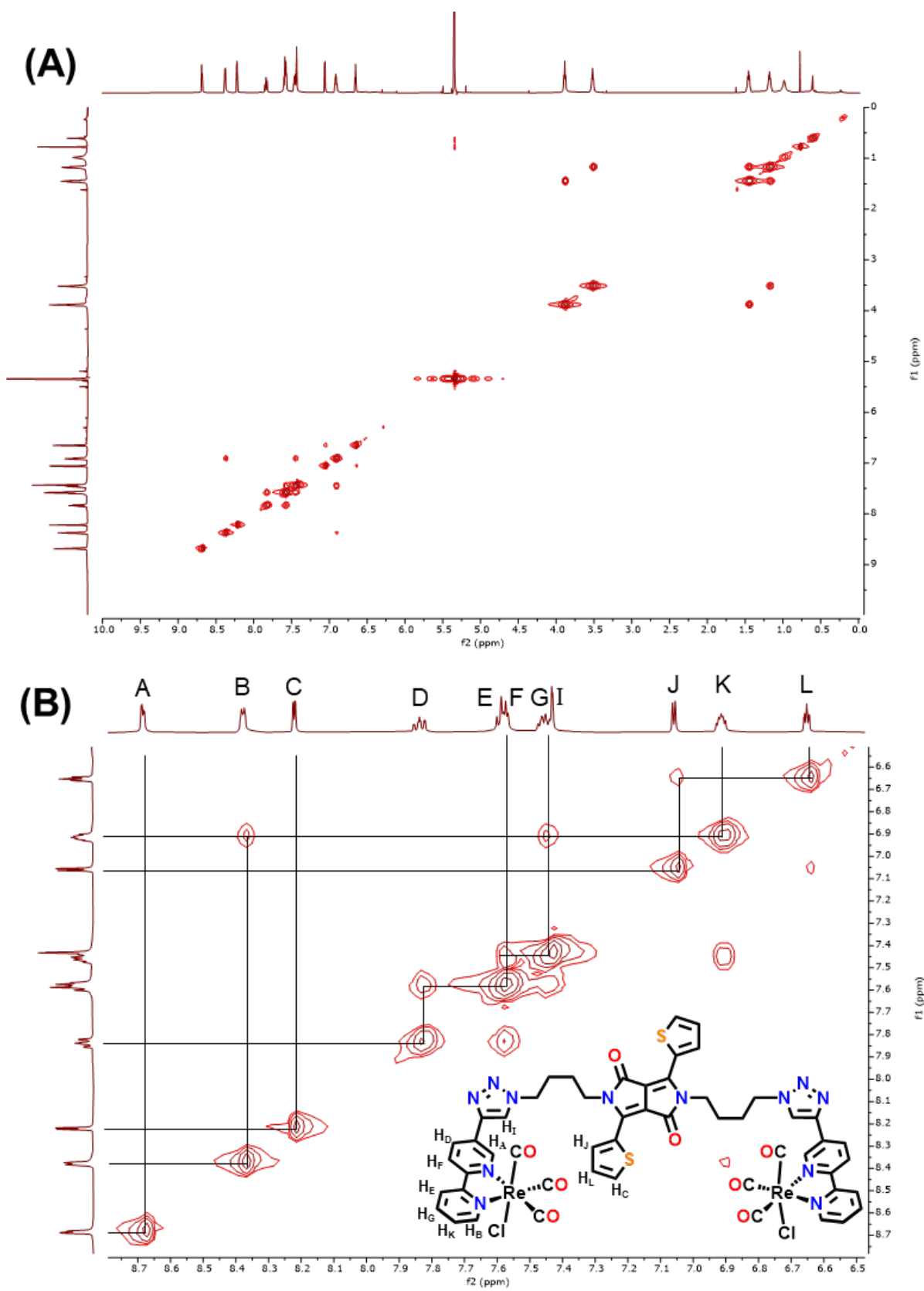
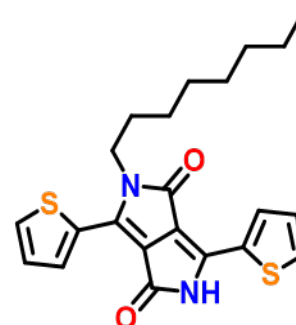
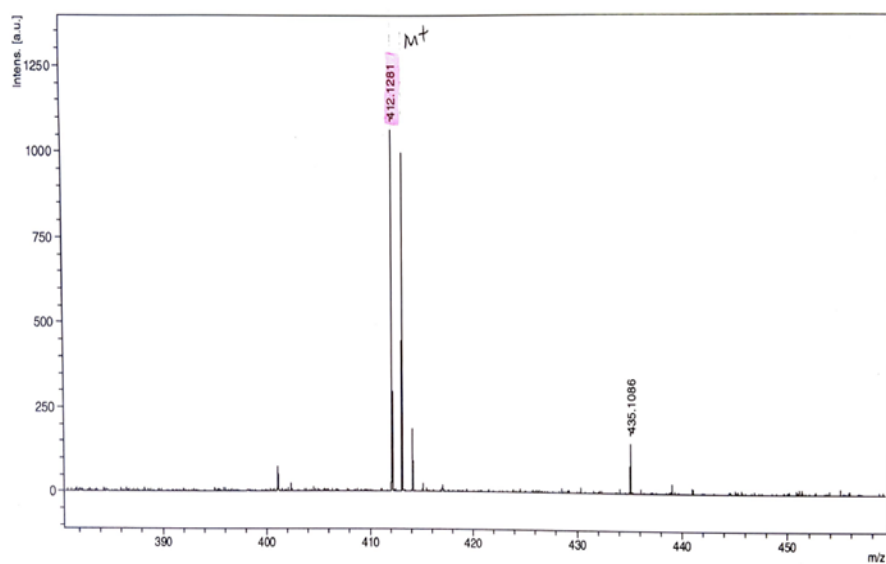


Figure S16. (A) Full ^1H - ^1H COSY spectrum with (B) enhanced view and assignment of aromatic protons for catalyst **2** (600 MHz, TCE- d_2)

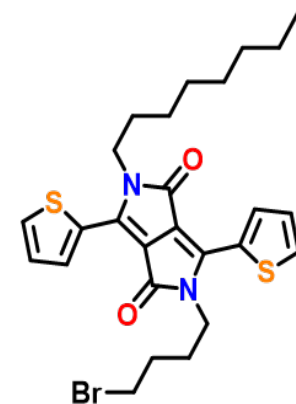
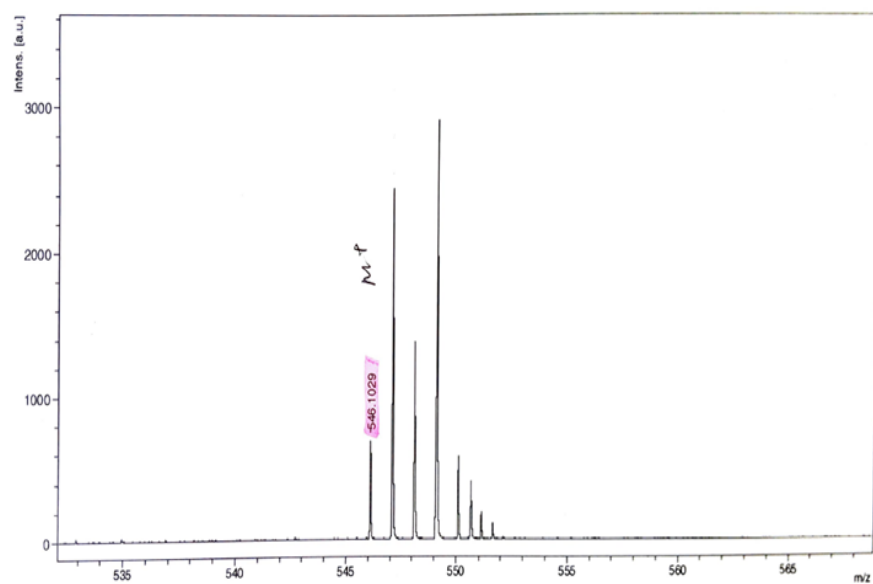
5. MALDI-TOF MS & CHN Elemental Analysis



Chemical Formula: $C_{22}H_{24}N_2O_2S_2$
Exact Mass: 412.13

$[M]^+ = 412.1274$

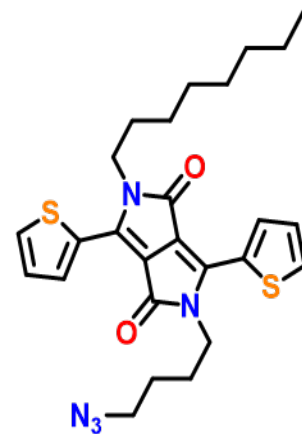
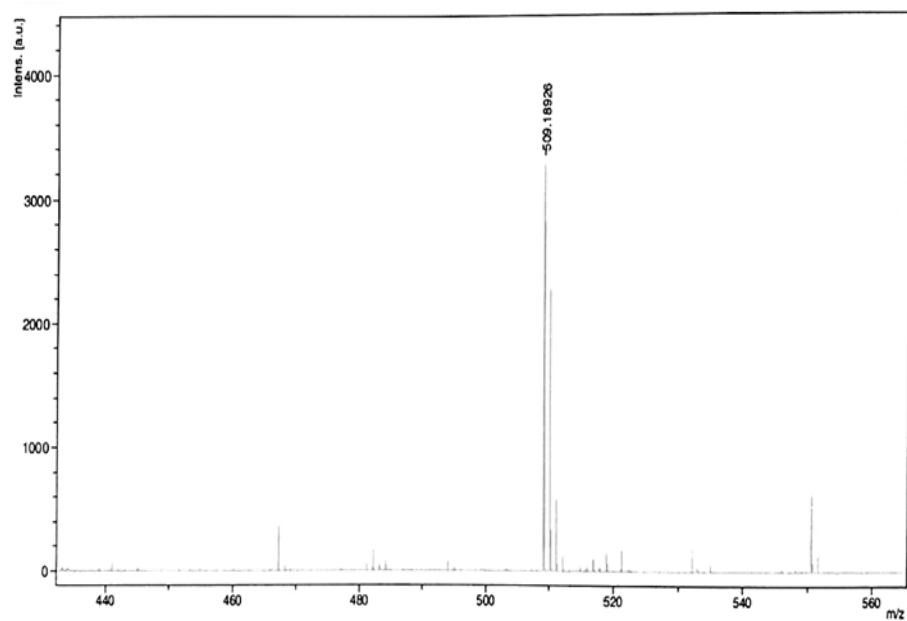
Figure S17. HR-MALDI-TOF mass spectrum of DPP-C8



Chemical Formula: $C_{26}H_{31}BrN_2O_2S_2$
Exact Mass: 546.10

$[M]^+ = 546.1005$

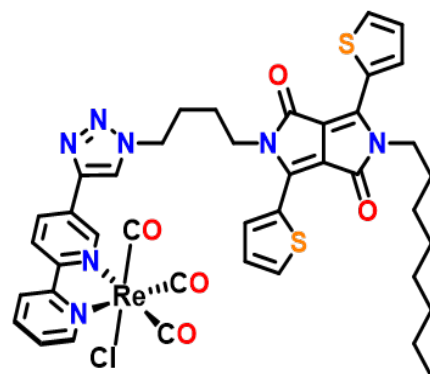
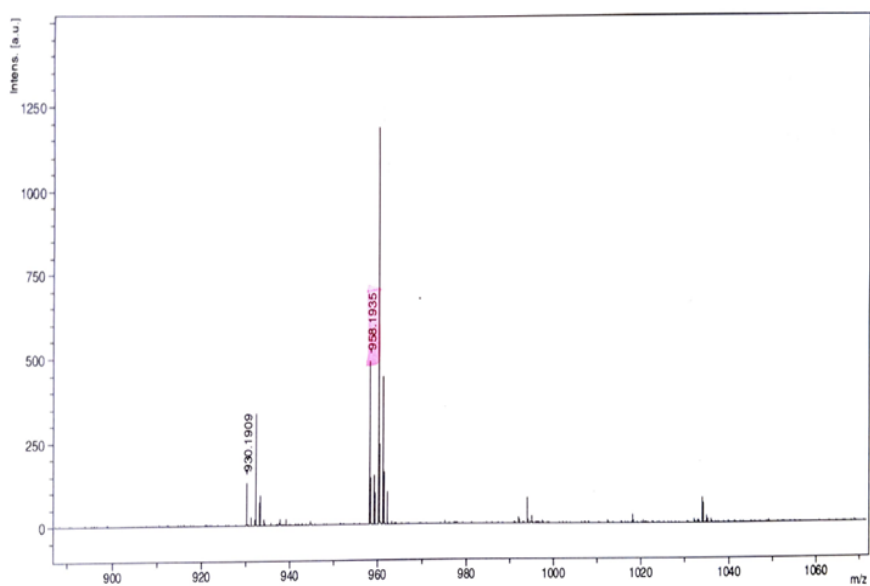
Figure S18. HR-MALDI-TOF mass spectrum of Br-C4-DPP-C8



Chemical Formula: $C_{26}H_{31}N_5O_2S_2$
 Exact Mass: 509.19

$[M]^+ = 509.1919$

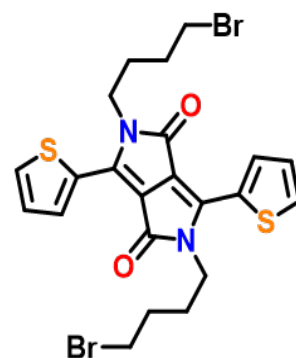
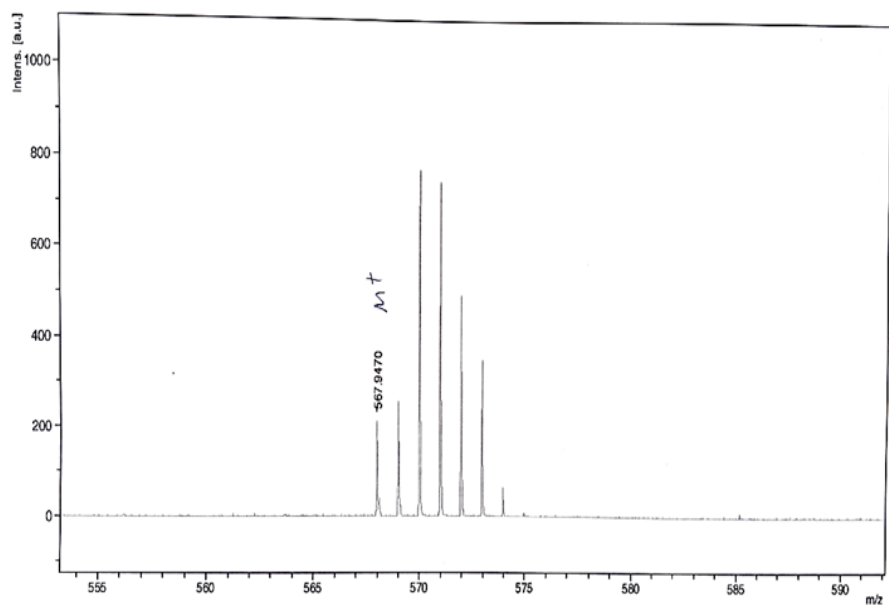
Figure S19. HR-MALDI-TOF mass spectrum of N_3 -C4-DPP-C8



Chemical Formula: $C_{41}H_{39}ClN_7O_5ReS_2$
 Exact Mass: 995.17

$[M-Cl]^+ = 958.1978$

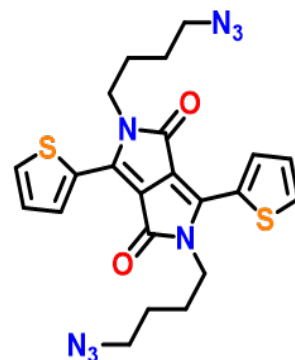
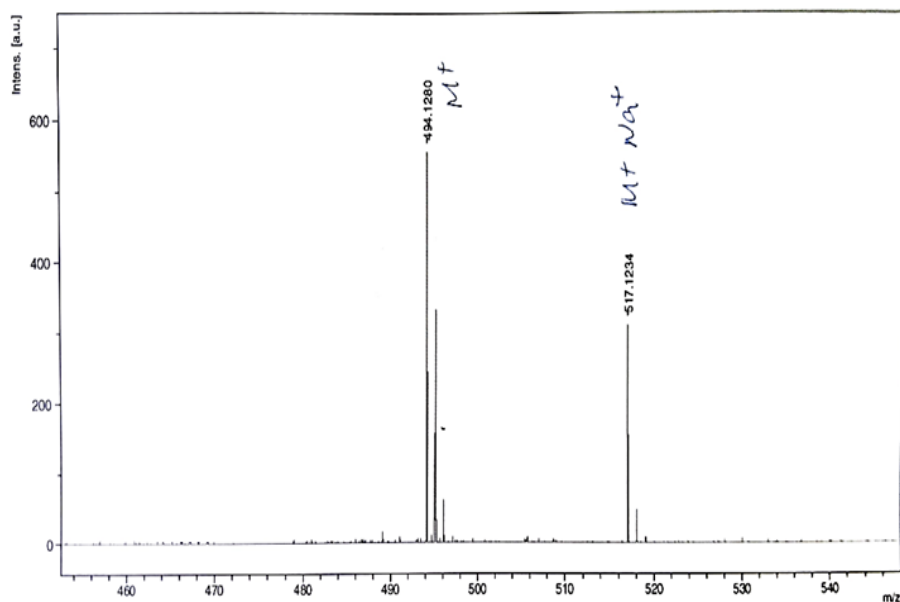
Figure S20. HR-MALDI-TOF mass spectrum of catalyst 1



Chemical Formula: $C_{22}H_{22}Br_2N_2O_2S_2$
 Exact Mass: 567.95

$[M]^+ = 567.9489$

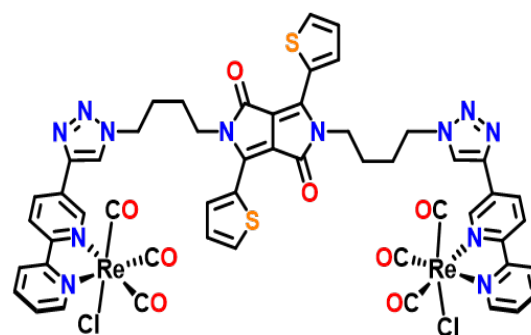
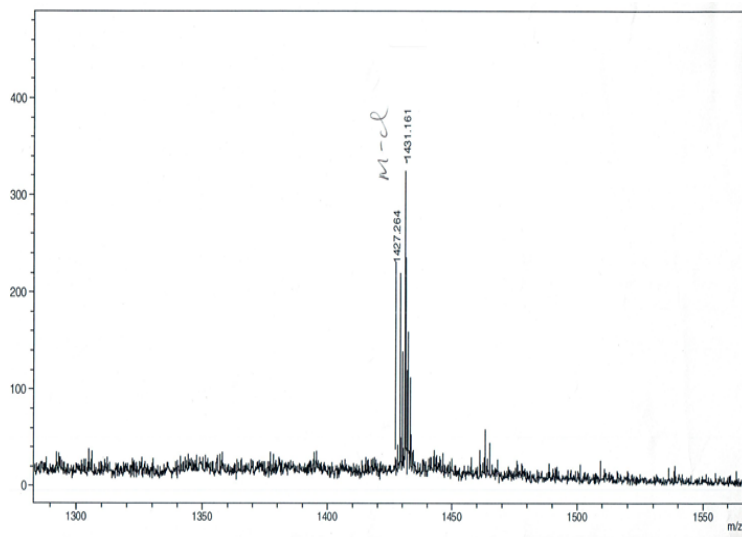
Figure S21. HR-MALDI-TOF mass spectrum of Br-C4-DPP-C4-Br



Chemical Formula: $C_{22}H_{22}N_8O_2S_2$
 Exact Mass: 494.13

$[M]^+ = 494.1307$

Figure S22. HR-MALDI-TOF mass spectrum of N₃-C4-DPP-C4-N₃



Chemical Formula: $C_{52}H_{38}Cl_2N_{12}O_8Re_2S_2$
Exact Mass: 1466.09

$[M-Cl]^+ = 1431.181$

Figure S23. HR-MALDI-TOF mass spectrum of catalyst 2

(A) University of Calgary
Department of Chemistry EA Date: 10/6/2021

Name:	JOSH	Group:	GW
Sample:	Re(bpy-DPP)	Weight (mg):	1.259
%C (Actual):	49.14	%C (Theoretical):	49.46
%H (Actual):	4.03	%H (Theoretical):	3.95
%N (Actual):	9.60	%N (Theoretical):	9.85

(B) University of Calgary
Department of Chemistry EA Date: 10/6/2021

Name:	JOSH	Group:	GW
Sample:	Re(bpy-DPP-bpy)Re	Weight (mg):	1.868
%C (Actual):	42.99	%C (Theoretical):	42.59
%H (Actual):	2.81	%H (Theoretical):	2.61
%N (Actual):	11.06	%N (Theoretical):	11.46

Figure S24. CHN elemental analyses of catalyst 1 (A) and catalyst 2 (B)

6. UV-Vis-nIR / FTIR Spectroscopies

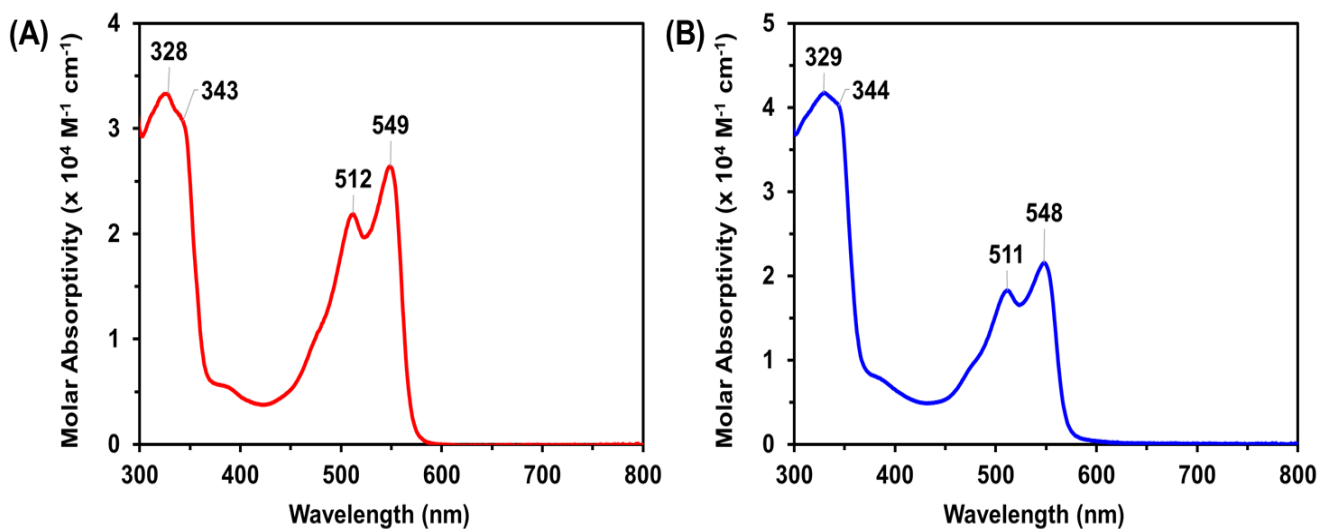


Figure S25. UV-vis absorbance spectra of catalysts **1** (A; red) and **2** (B; blue) in DMF ($\sim 10^{-5} \text{ M}$)

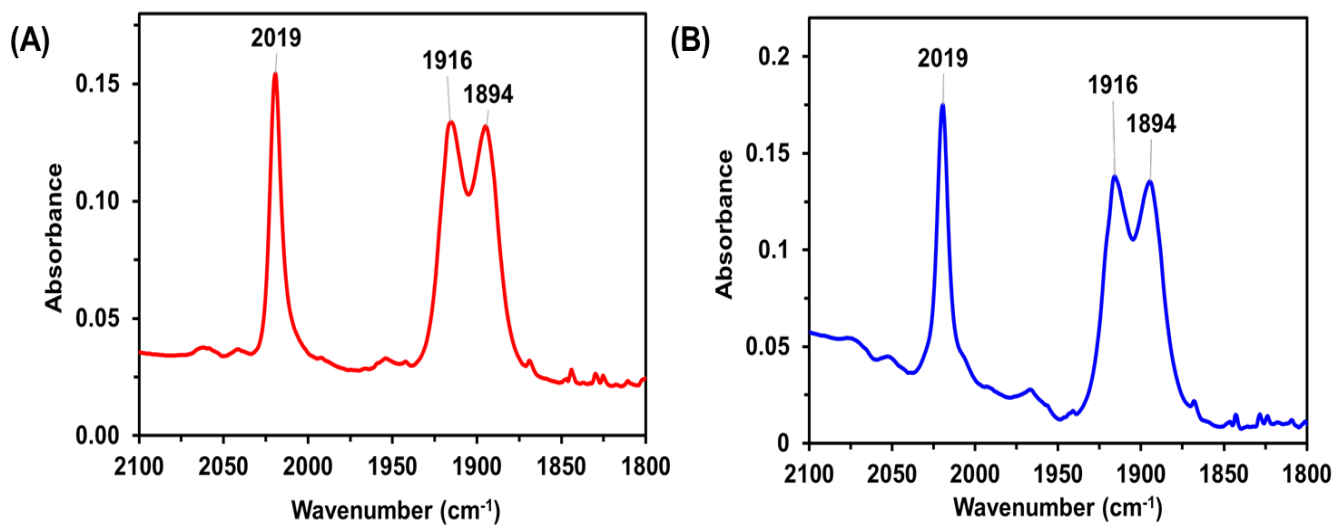


Figure S26. FTIR absorbance spectra of catalysts **1** (A; red) and **2** (B; blue) in DMF ($\sim 10^{-3} \text{ M}$)

7. Electrochemistry Under Argon and CO₂

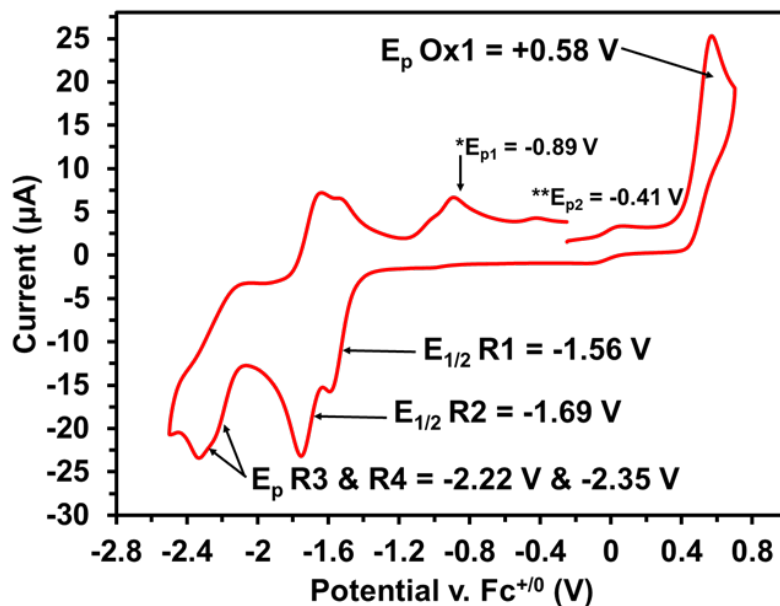


Figure S27. Cyclic voltammogram of catalyst 1. All measurements were recorded at 100 mV/s, under argon in CH₂Cl₂ with 0.1 M TBAPF₆ supporting electrolyte (WE = glassy carbon, CE = Pt-wire, RE = Ag/AgCl, and Fc⁺⁰ as internal reference standard)

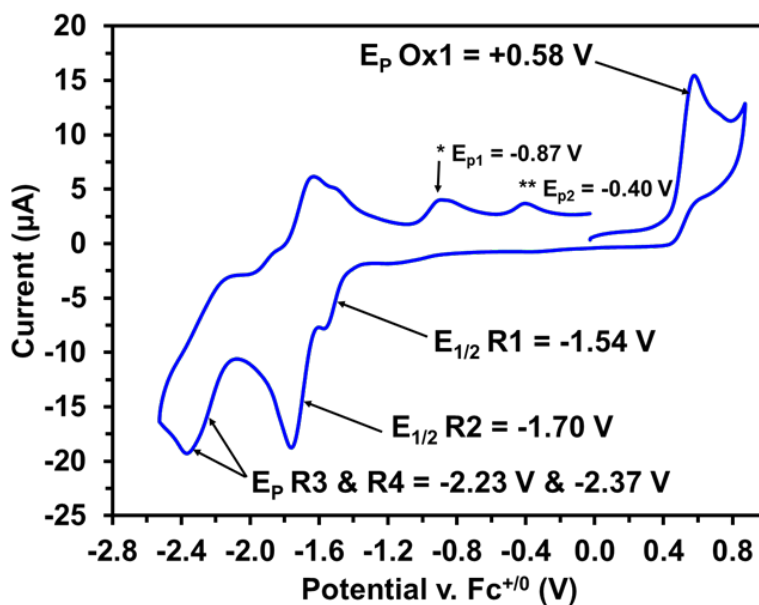


Figure S28. Cyclic voltammogram of catalyst 2. All measurements were recorded at 100 mV/s, under argon in CH₂Cl₂ with 0.1 M TBAPF₆ supporting electrolyte (WE = glassy carbon, CE = Pt-wire, RE = Ag/AgCl, and Fc⁺⁰ as internal reference standard)

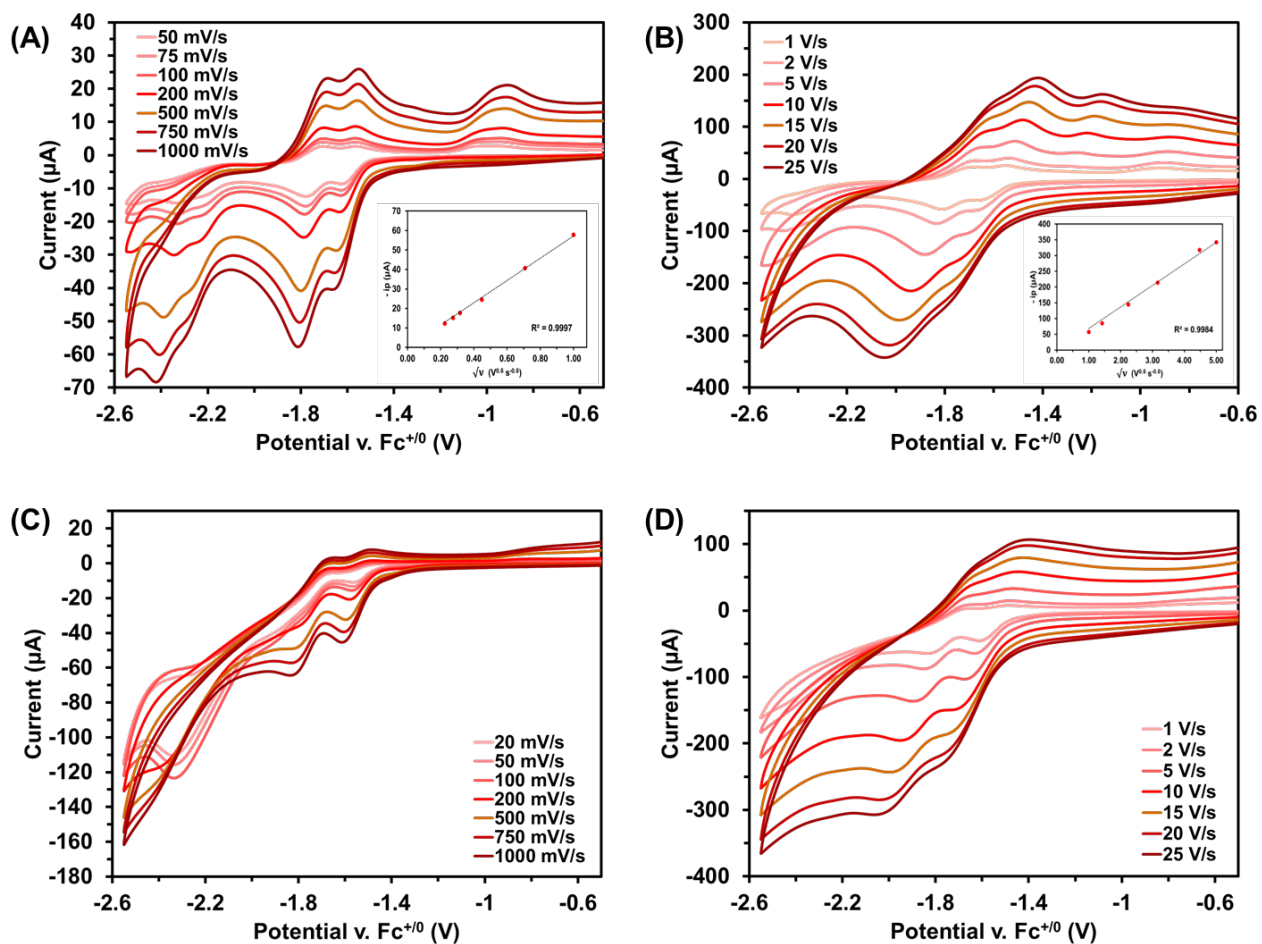


Figure S29. CVs of catalyst **1** recorded at variable scan rate under argon (A and B) and under CO_2 (C and D) in DMF with 0.1 M TBAPF_6 supporting electrolyte (WE = glassy carbon, CE = Pt-wire, RE = Ag/AgCl, and $\text{Fc}^{+/0}$ as internal reference standard). Under argon, linear fitting of the scan rate to the Randles-Sevcik equation (inset graphs of A and B) demonstrates that **1** undergoes a diffusion-limited current response, with $D = 4.9 \times 10^{-6} \text{ cm}^2 \text{ s}^{-1}$

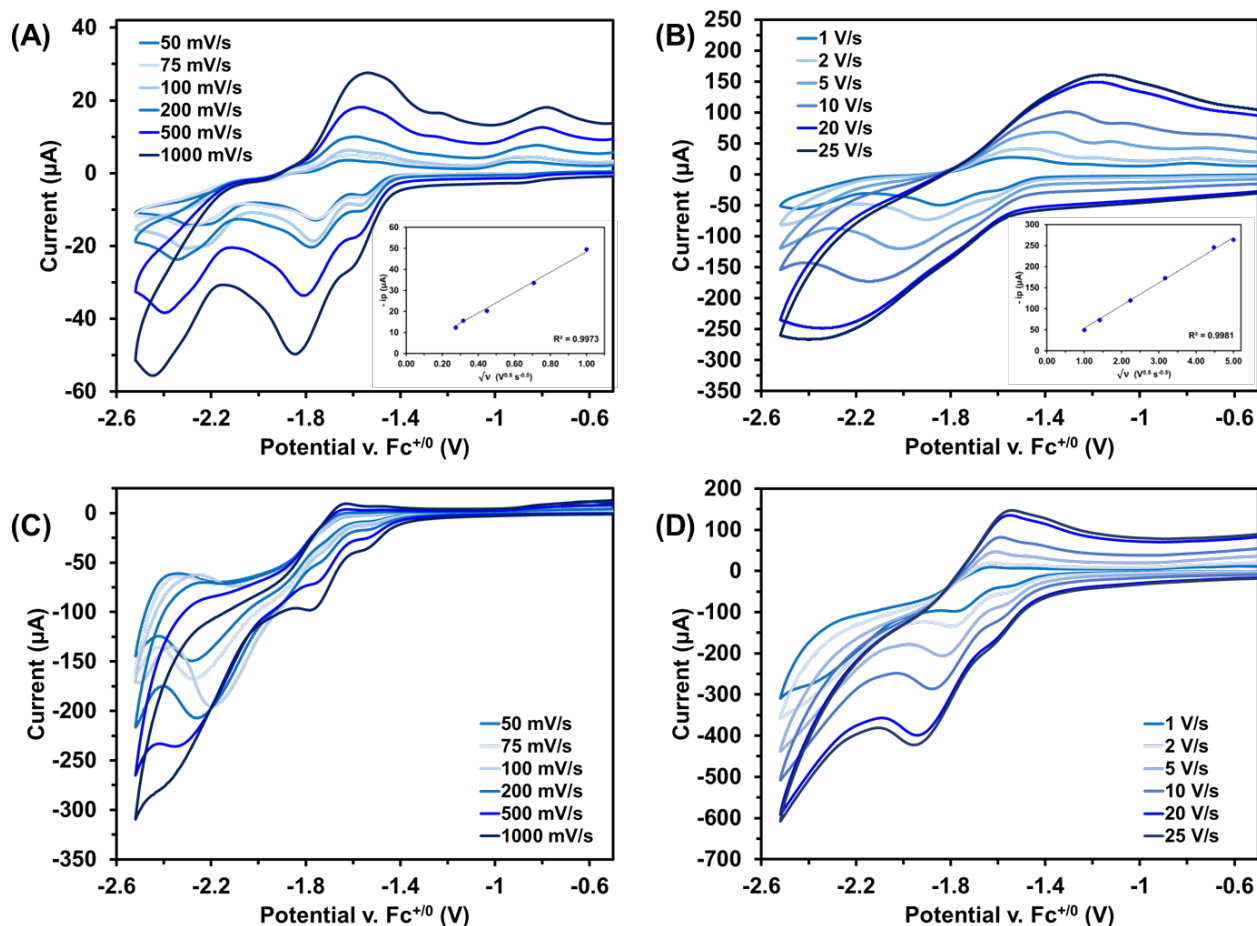


Figure S30. CVs of catalyst **2** recorded at variable scan rate under argon (A and B) and under CO₂ (C and D) in DMF with 0.1 M TBAPF₆ supporting electrolyte (WE = glassy carbon, CE = Pt-wire, RE = Ag/AgCl, and Fc⁺⁰ as internal reference standard). Under argon, linear fitting of the scan rate to the Randles-Sevcik equation (inset graphs of A and B) demonstrates that **2** undergoes a diffusion-limited current response, with $D = 7.9 \times 10^{-6} \text{ cm}^2 \text{ s}^{-1}$

8. Electro-/Photocatalytic Experiments

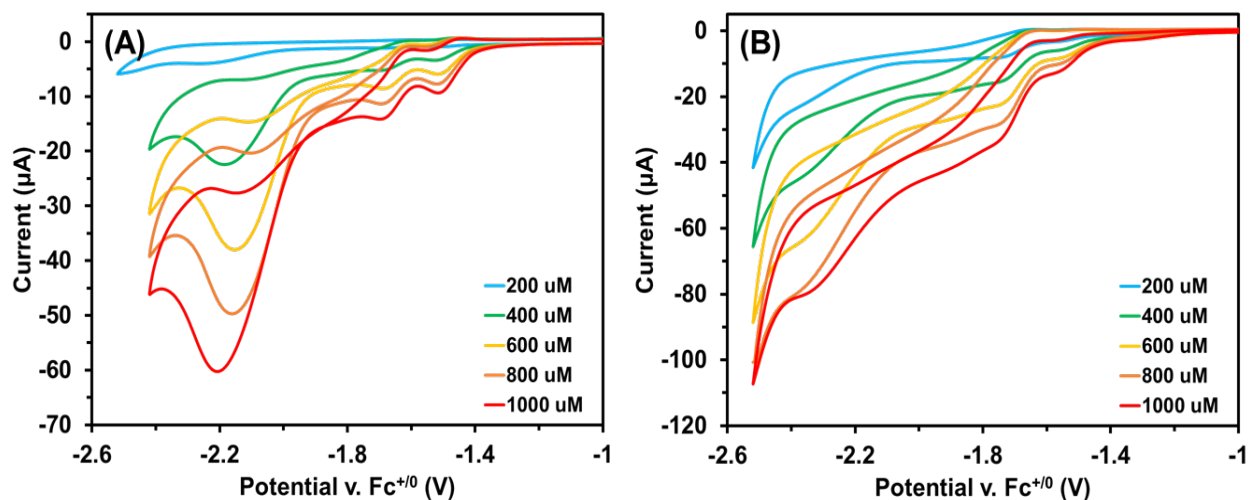


Figure S31. CV current enhancement effects as a function of catalyst 1 (A) and catalyst 2 (B) concentration. Under an atmosphere of CO₂, CVs of each catalyst were measured at 0.2 mM (blue), 0.4 mM (green), 0.6 mM (yellow), 0.8 mM (orange), and 1.0 mM (red) were. All measurements were recorded at 100 mV/s, in DMF with 1 M TFE and 0.1 M TBAPF₆ supporting electrolyte (WE = glassy carbon, CE = Pt-wire, RE = Ag/AgCl, and Fc⁺⁰ as internal reference standard). Both catalyst 1 and catalyst 2 show a linear increase in current enhancement as a function of catalyst concentration, consistent with a first-order rate-dependence

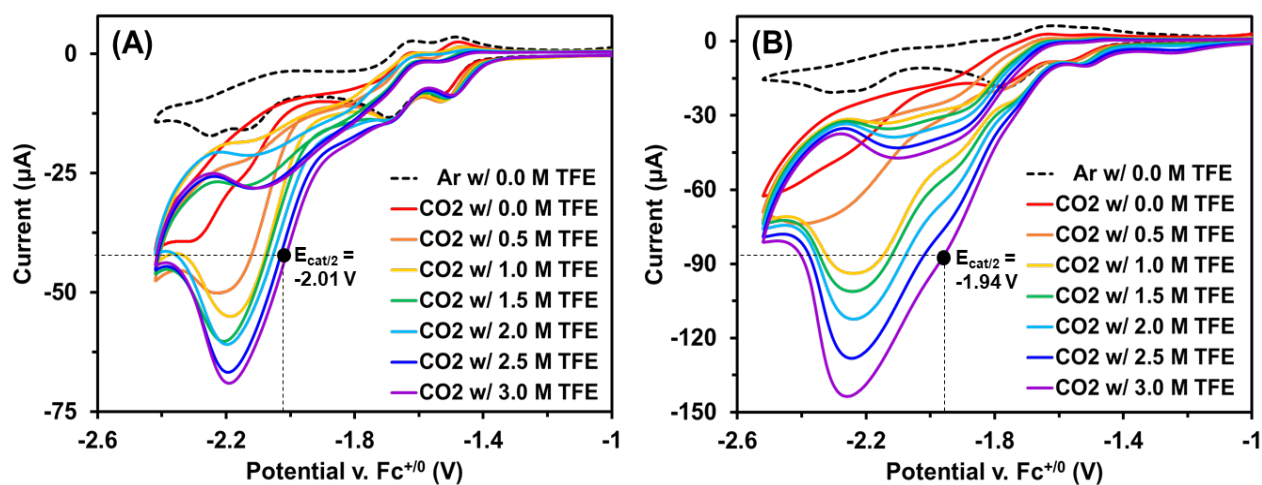


Figure S32. CV current enhancement plots as a function of 2,2,2-trifluoroethanol (TFE) concentration for catalyst 1 (A) and catalyst 2 (B). TFE was incrementally added at 0 M (red), 0.5 M (orange), 1.0 M (yellow), 1.5 M (green), 2.0 M (light blue), 2.5 M (dark blue), and 3.0 M (purple). All measurements were recorded at 100 mV/s, under an atmosphere of CO₂, in DMF with 0.1 M TBAPF₆ supporting electrolyte (WE = glassy carbon, CE = Pt-wire, RE = Ag/AgCl, and Fc⁺⁰ as internal reference standard). Current enhancement is expected to be proportional to the square-root of TFE concentration, so the linear dependence observed indicates second-order rate dependence on the proton source for catalyst 1 and catalyst 2

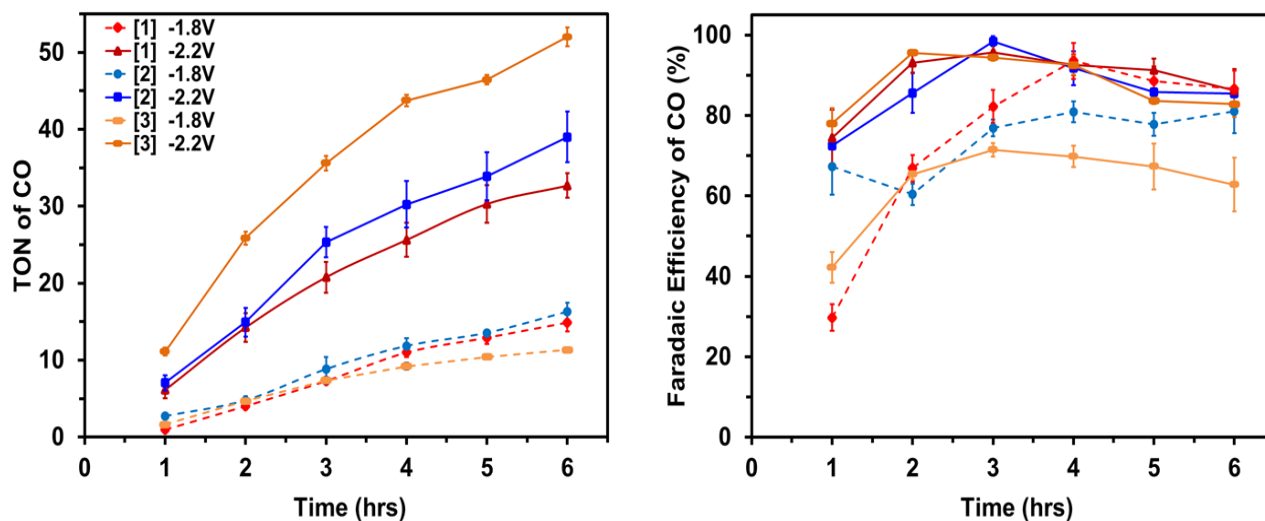


Figure S33. Comparing average TON_{CO} (A) and Faradaic efficiencies of CO formation (B) achieved by catalysts **1** (red), **2** (blue), and **3** (orange) during CPE experiments in 0.1 M TBAPF₆ in DMF saturated with CO₂ at an applied potential of -1.8 vs. Fc⁺⁰ (dashed line) and -2.2 vs. Fc⁺⁰ (solid line)

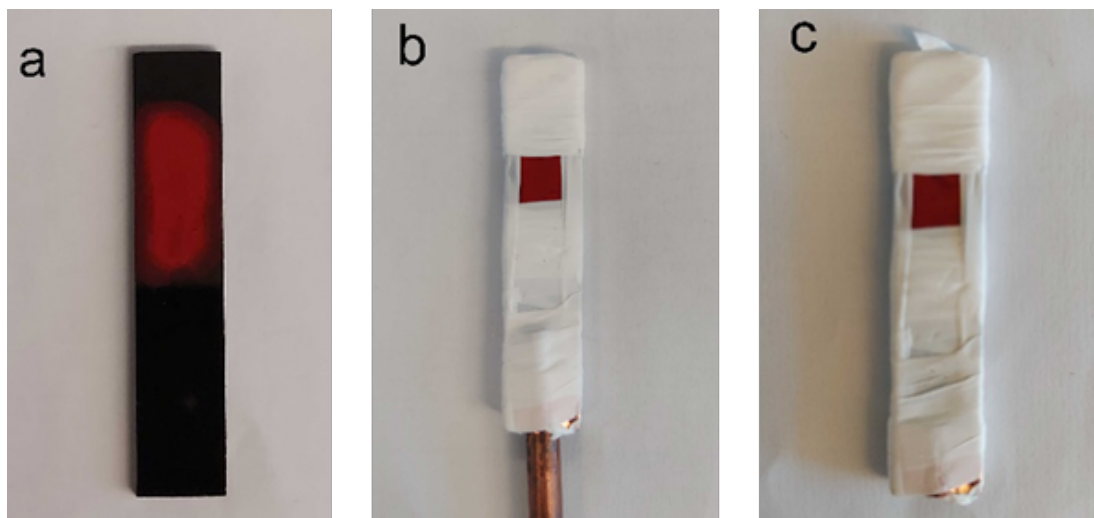


Figure S34. Representative glassy carbon electrode fabrication with **2** drop casted onto glassy carbon. (a) after drying for 24 hours in ambient air, (b) wrapped with PTFE pre-electrolysis, (c) post-electrolysis; geometric area of film in (b-c) is 36 mm². $\text{FE}_{\text{CO}}\%$ of 34%

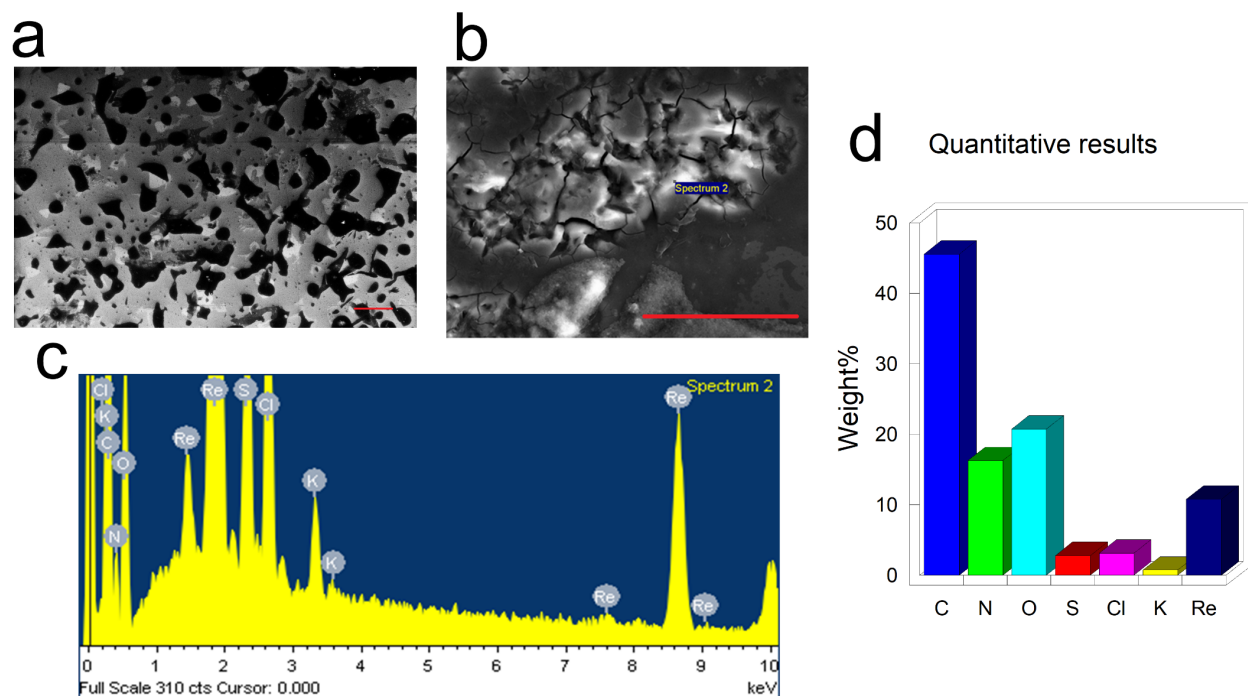


Figure S35. SEM images of films made by drop casting 1 mM DMF solution of **2** onto glassy carbon. (a) SEM image collected at 10 keV of film (b) SEM image collected at 20 keV; red bar indicates 100-micron, both images collected with SE2 detector (c) EDX spectrum of the film, (d) relative weight% by element in the outer ring region. FE_{CO} of 34%

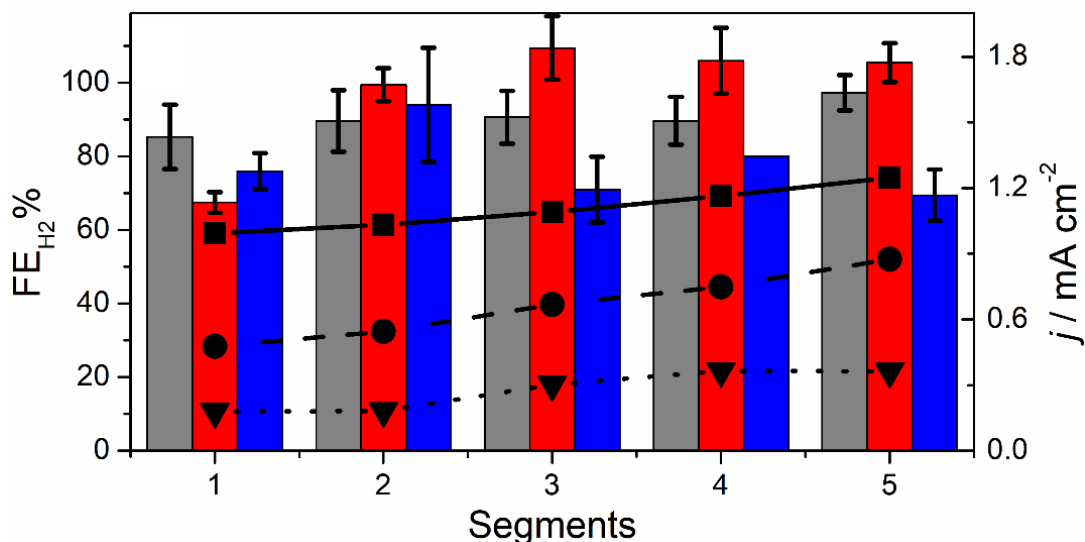


Figure S36. H₂ evolved during CPE at -0.75 V vs RHE quantified by GC-PDHID. CPE at -0.75 V vs RHE colored bars are FE% for H₂ and line are current density; grey bars and circles are carbon paper, blue bars and triangles are PDPPTD coating on carbon paper, and red bars and squares are CIC-85 on carbon paper. All solutions are 0.5 M KHCO₃ under CO₂ (pH = 7.4); 1 segment = 30 min of continuous electrolysis

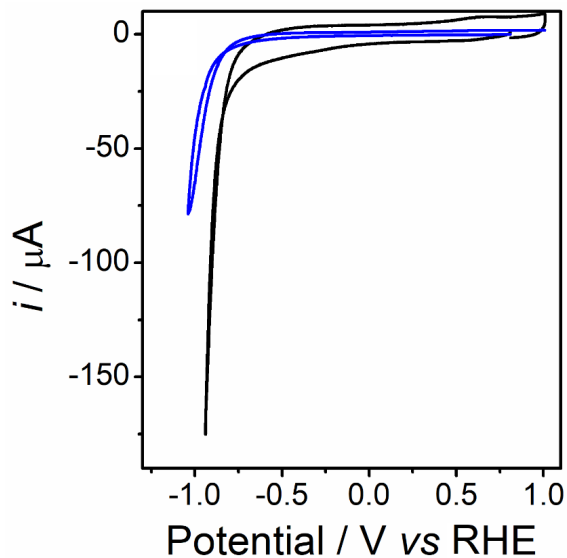


Figure S37. CV of 1 cm² carbon paper (black) and PDPPPTD coated carbon paper (blue)

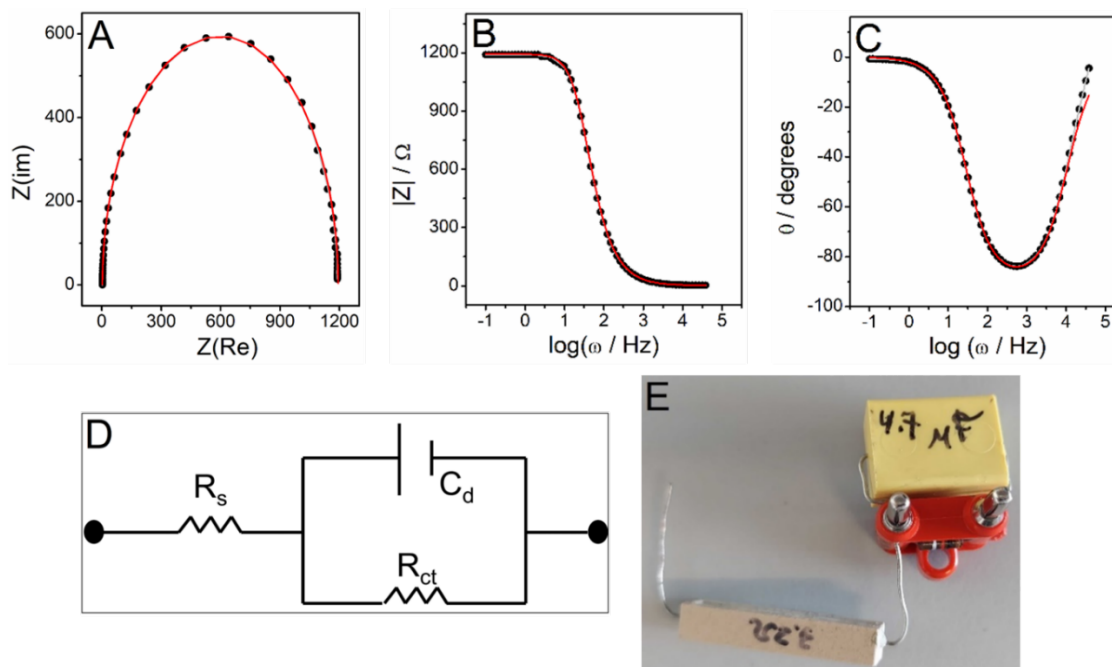


Figure S38. EIS of dummy Randle cell measured at open circuit potential. (A) Nyquist plot and Bode plots of (B) impedance versus radial frequency and (C) phase shift angle versus radial frequency. Black dots are data, grey line is Kramers-Kronig fit ($\chi^2 = 0.000345$), and red line is circuit fit ($\chi^2 = 0.122$). (D) Circuit model $R_s = 3.2 \Omega$, $R_{ct} = 1.2 \text{ k}\Omega$, and $C_d = 4.7 \mu\text{F}$. (E) Image of dummy Randle cell with independently measured components $R_s = 3.2 \Omega$, $R_{ct} = 1.2 \text{ k}\Omega$, and $C_d = 4.7 \mu\text{F}$

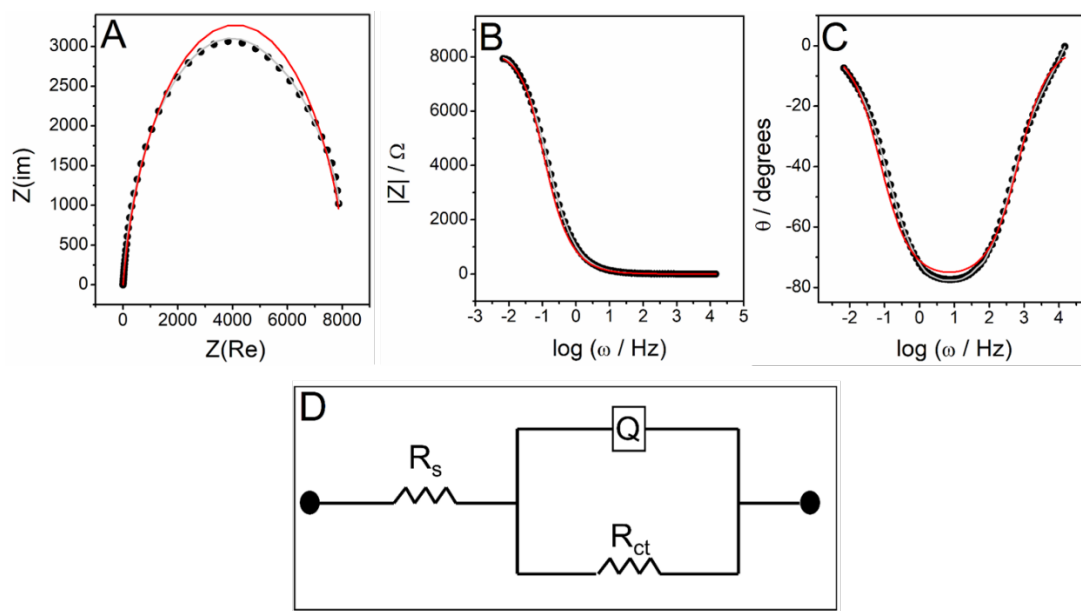


Figure S39. EIS of carbon paper in aqueous 0.5 M KHCO_3 ($\text{pH} = 7.4$) at 0.1 V vs RHE. (A) Nyquist plot, and Bode plots: (B) impedance versus radial frequency and (C) phase shift angle versus radial frequency. Black dots are data, grey line is Kramers-Kronig fit ($\chi^2 = 0.00279$), and red line is circuit fit ($\chi^2 = 0.66$). (D) Circuit model $R_s = 3.3 \Omega$, $R_{ct} = 8.2 \text{ k}\Omega$, and $Q = 233 \mu\text{S}^\circ$, $\alpha = 0.85$

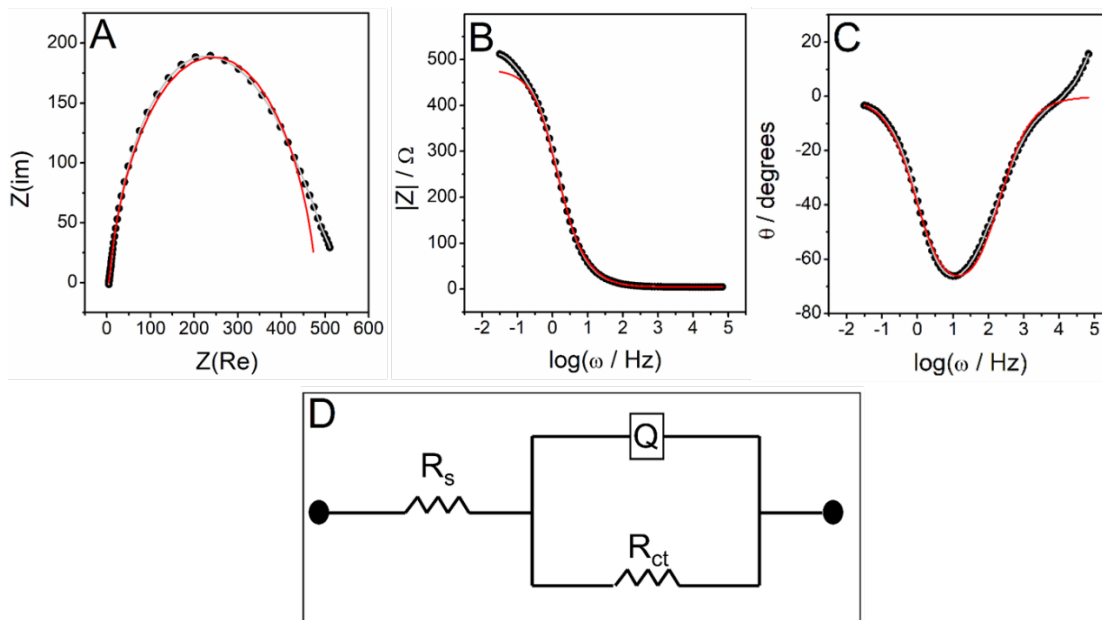


Figure S40. EIS of carbon paper coated with PDPPTD in aqueous 0.5 M KHCO_3 ($\text{pH} = 7.4$) at 0.1 V vs RHE. (A) Nyquist plot, and Bode plots: (B) impedance versus radial frequency and (C) phase shift angle versus radial frequency. Black dots are data, grey line is Kramers-Kronig fit ($\chi^2 = 0.014$), and red line is circuit fit ($\chi^2 = 0.39$). (D) Circuit model $R_s = 4.5 \Omega$, $R_{ct} = 0.48 \text{ k}\Omega$, and $Q = 476 \mu\text{S}^\circ$, $\alpha = 0.85$

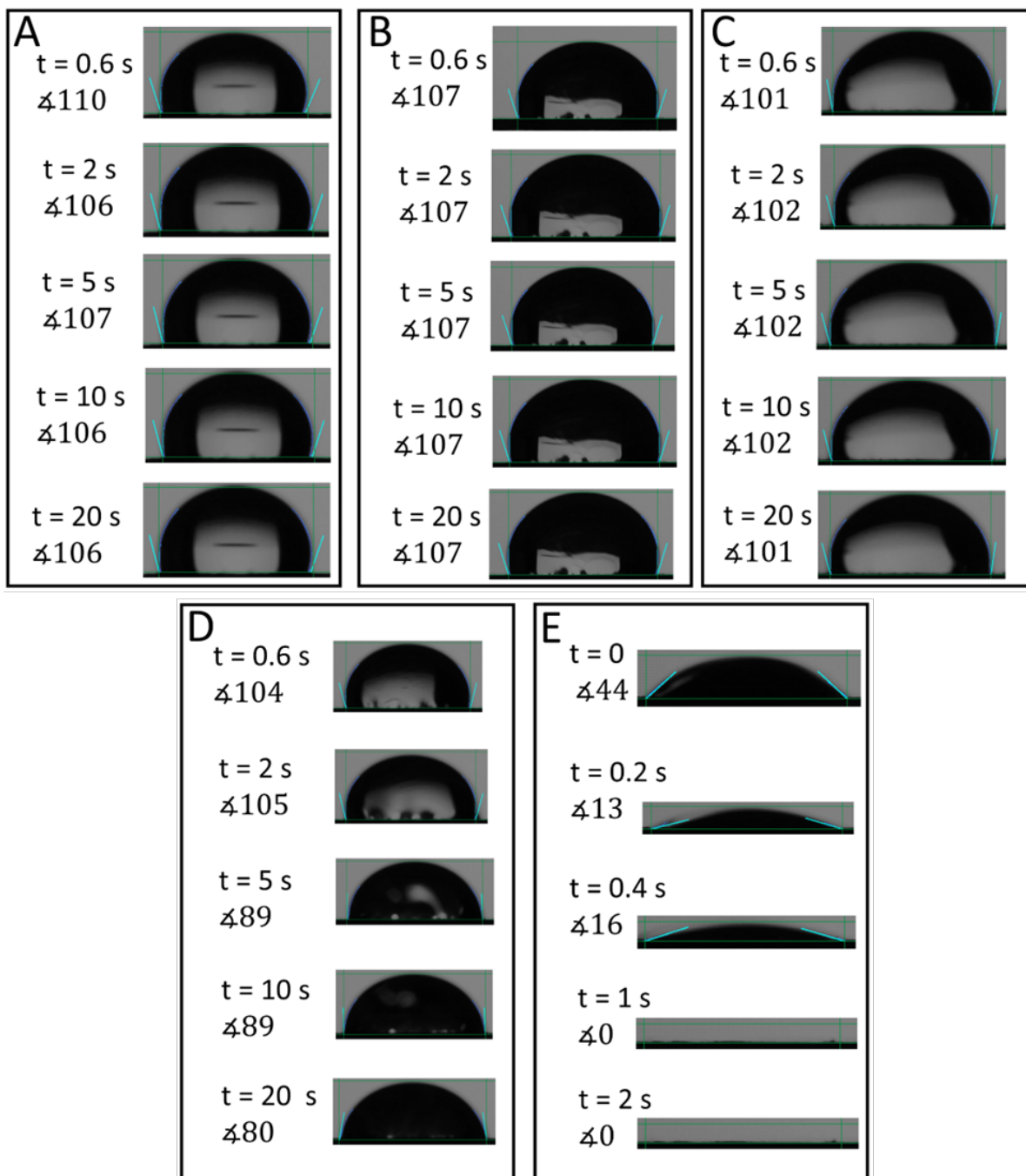


Figure S41. Contact angles measured with aqueous 0.5 M KHCO_3 (pH = 8.5) electrolyte over a incremental time intervals from 0.6 s of droplet contact up to 20 seconds; time and angle measured appear on the left side of each image. (A) carbon paper, (B) 2 on carbon paper (C) PDPPPTD on carbon paper, (D) CIC-85 on carbon paper, (E) CIC-85 on PDPPPTD on carbon paper

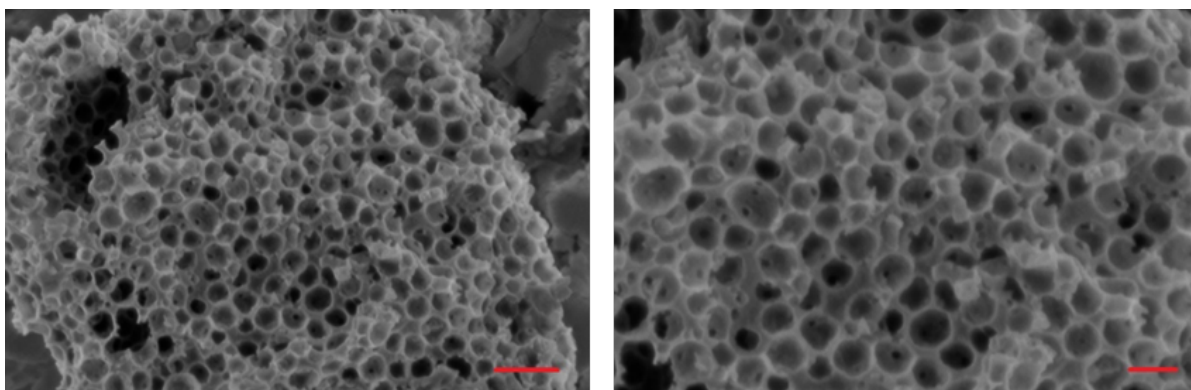


Figure S42. SEM image of CIC-85. (left) at 1 keV with Inlens detector, red bar is 200 nm. (right) at 1 keV with Inlens detector, red bar is 100 nm

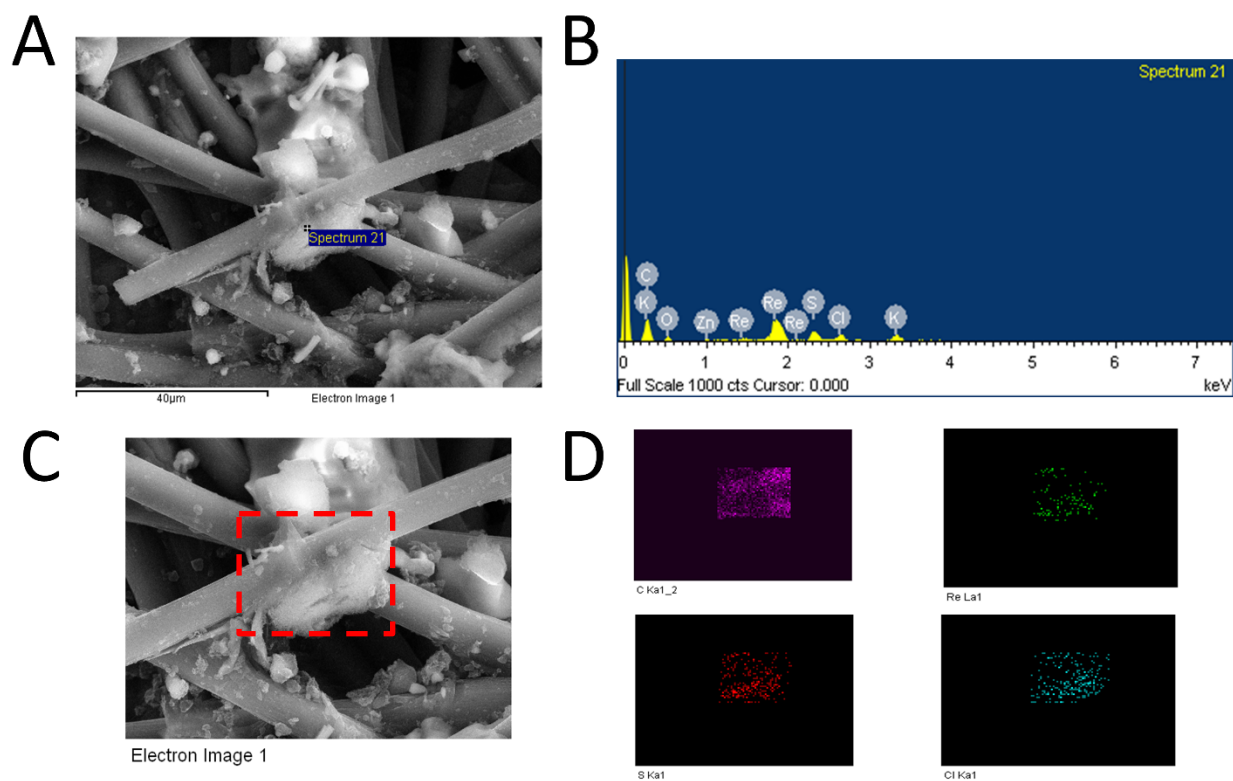


Figure S43. SEM-EDX of **2** on CIC on PDPPPTD on carbon paper. (A) SEM image collected at 20 keV with SE2 detector with target area shown. (B) EDX spectrum of target area shown in image. (C) SEM image as shown in A with red box denoting region of interest. (D) EDX mapping of image drawn as red box showing distribution of Re (green), S (red), Cl (teal), and C (pink)

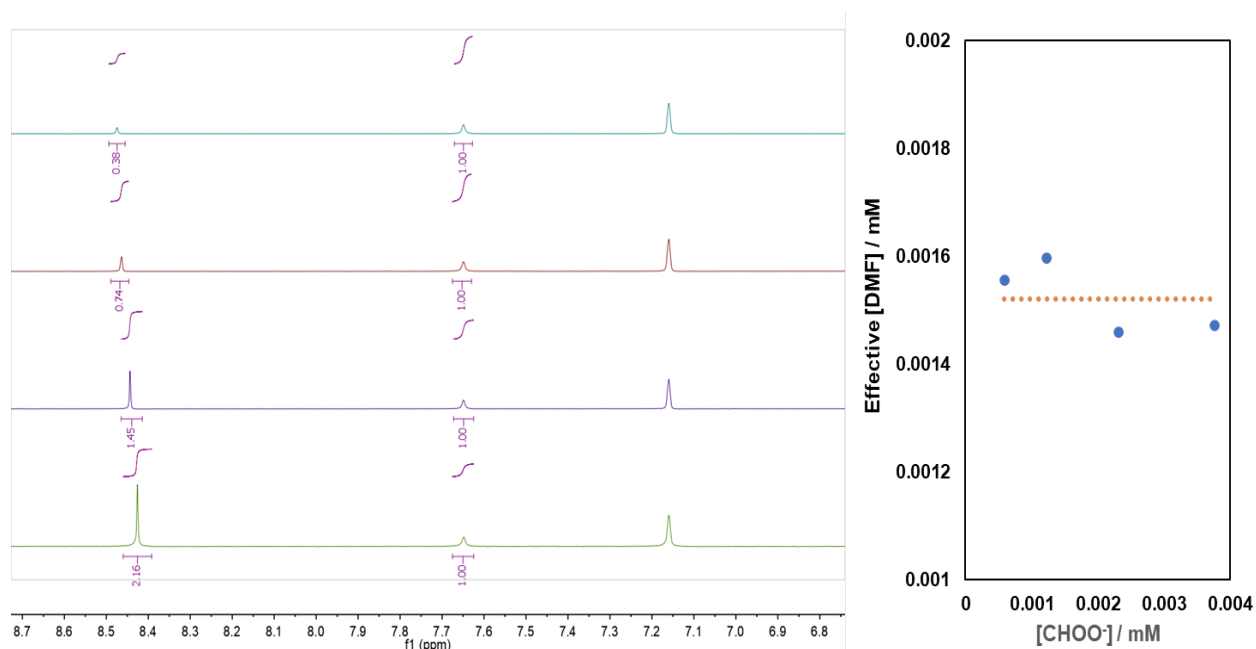


Figure S44. Calibration of DMF concentration in capillary with C_6D_6 by quantitative NMR. (Left) Integrated 1H -NMR spectra of varied amounts of sodium formate dissolved in 0.5 M $KHCO_3$ (pH = 8.5) solution. (Right) Plot of DMF concentration C_6D_6 determined from dissolved sodium formate in 0.5 M $KHCO_3$ (pH = 8.5) solution; $[DMF]_{eff} = 0.00152 \pm 0.00007$ mM

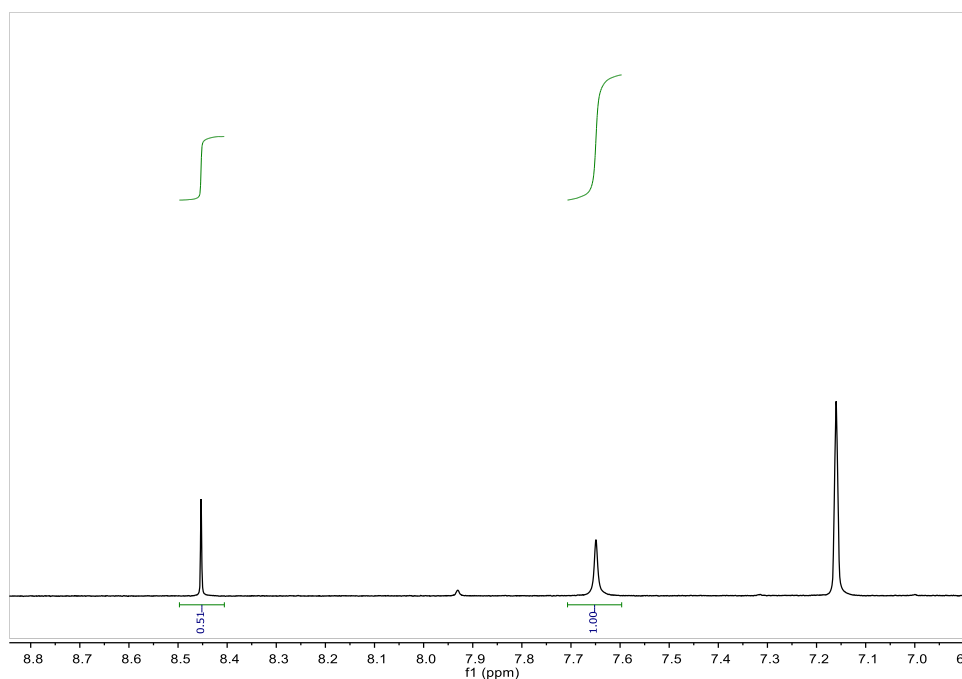


Figure S45. Quantitative 1H -NMR spectrum of post-CPE solution of **2** on carbon paper in 0.5 M $KHCO_3$ (pH = 7.4) solution with standardized DMF in C_6D_6 contained within capillary. Charge consumed during CPE was 55 C equating to a FE of 0.2% with regards to formate

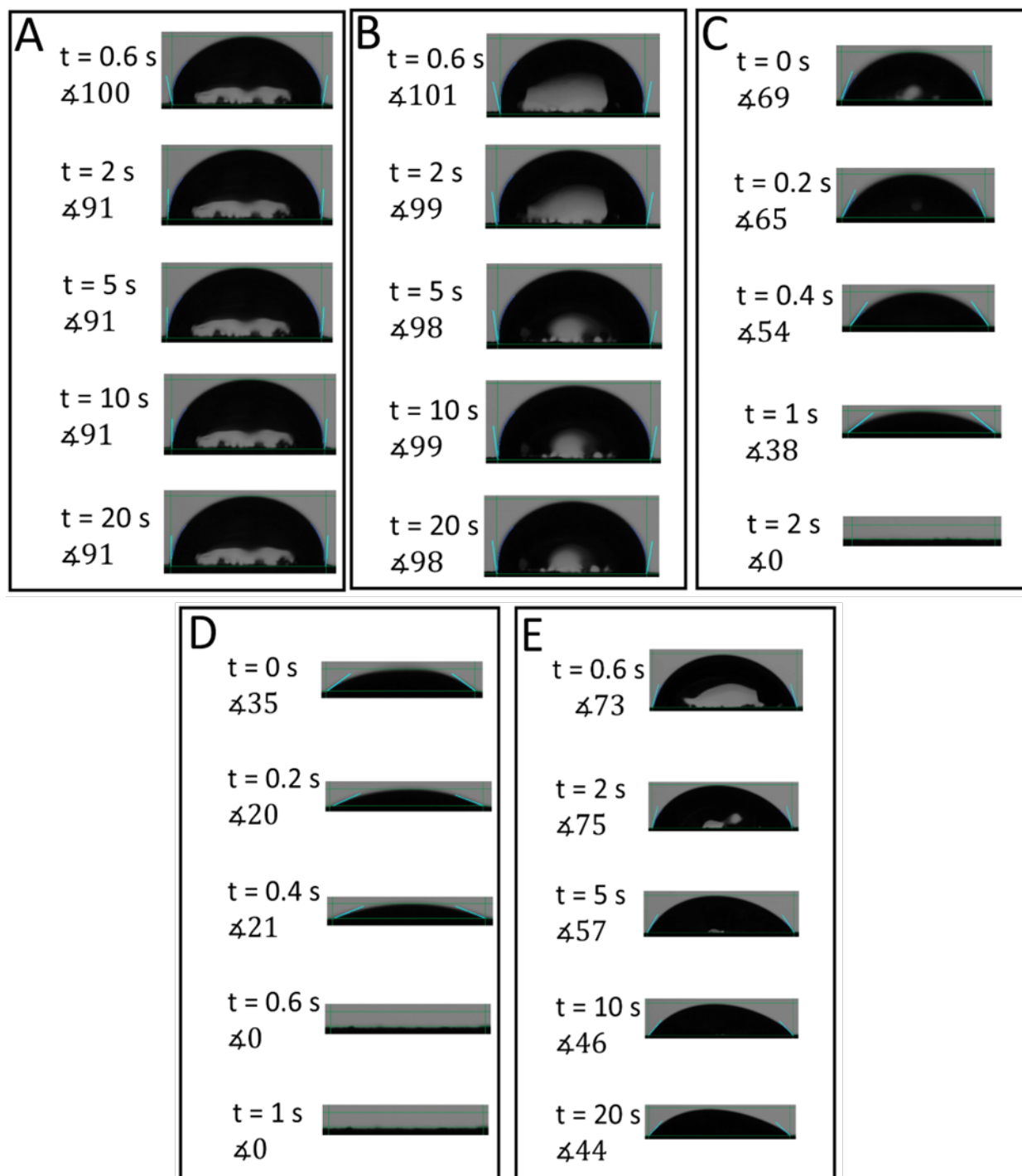


Figure S46. Contact angles measured with aqueous 0.5 M KHCO_3 (pH = 8.5) electrolyte over an incremental time intervals from 0 s of droplet contact up to 20 seconds or shortly after a breakthrough event; time and angle measured appear on the left side of each image. (A) **2** on PDPPPTD on carbon paper, (B) **2** on CIC on carbon paper, (C) **2** on CIC on PDPPPTD on carbon paper, (D) **1** on CIC on PDPPPTD on carbon paper, (E) **3** on CIC on PDPPPTD on carbon paper

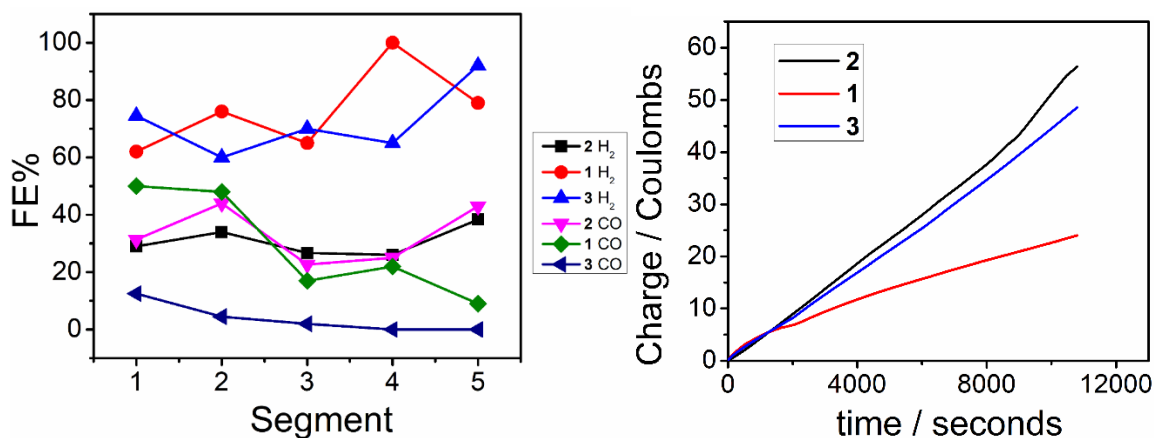


Figure S47. CPE at an applied potential of -0.75 V vs RHE with **1**, **2**, and **3** on CIC-85 on PDPPPTD on carbon paper *i.e.* catalyst/polymer/CIC shown in main text as Figure 7. (left) FE% for H₂ and CO measured over time. 1 segment = 30 min of continuous electrolysis. (right) representative charge versus time plots.

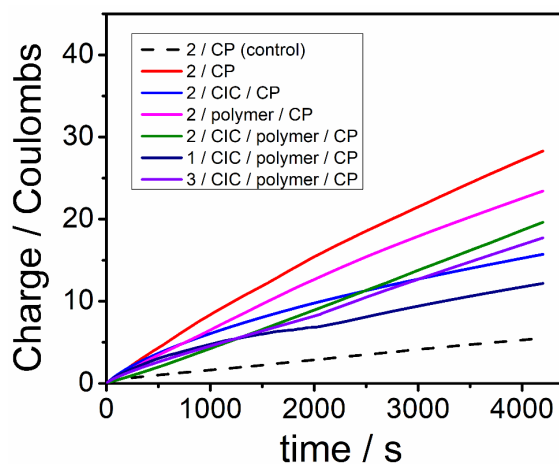


Figure S48. Representative charge versus time plots of CPEs performed at -0.75 V vs RHE in aqueous 0.5 M KHCO_3 ($\text{pH} = 7.4$) electrolyte; control is aqueous 0.5 M $\text{HPO}_4^{2-}/\text{H}_2\text{PO}_4^-$ ($\text{pH} = 7.4$). FE% and j can be found in the main text Figure 7.

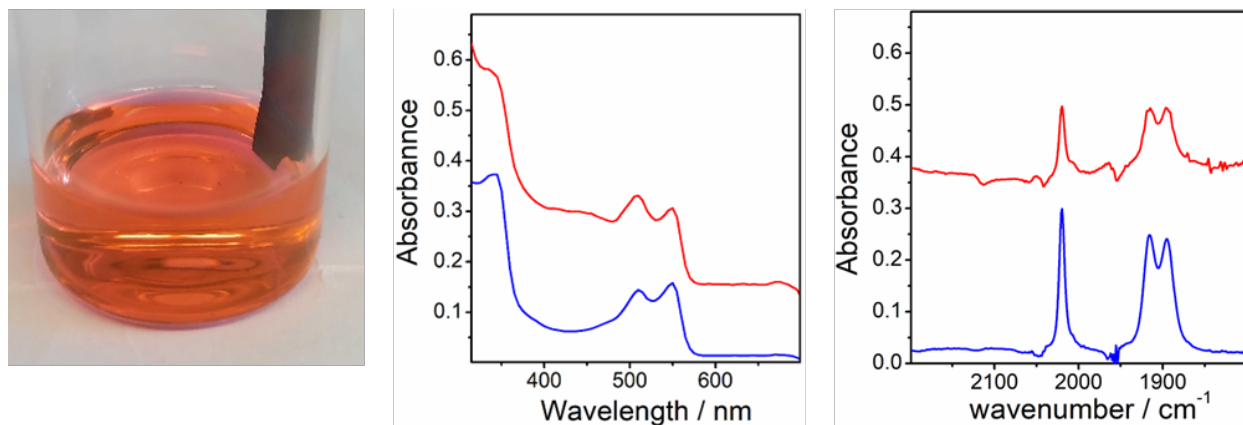


Figure S49. (Left) Representative solution of **1** and **2** from the desorption of carbon paper electrode in DMF post CPE; solution diluted by a factor of 1:100 for spectral analysis. (middle) UV-Vis spectrum of **1** and **2** in DMF post CPE, red (off-set on y-axis) and blue, respectively. (right) IR spectrum of **1** and **2** in DMF post CPE, red (off-set on y-axis) and blue, respectively

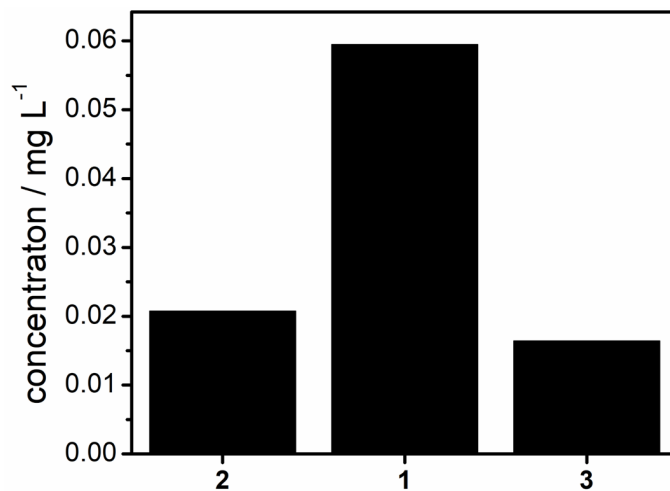


Figure S50. Concentrations of [Re] in post-CPE solutions of 0.5 M KHCO₃ (pH = 7.4) by ICP-MS analysis. Amount of [Re] in a 20 mL CPE solution equates to less than 0.03% of the original 4 μmol of catalyst introduced to carbon paper by drop casting

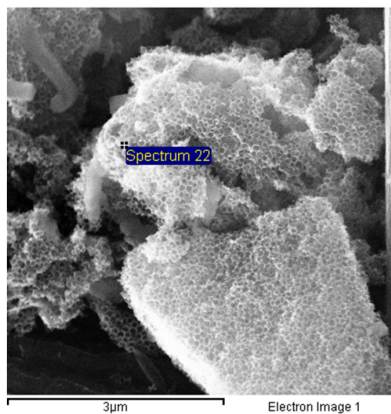
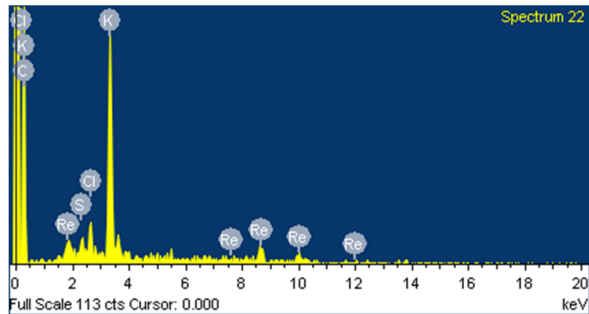
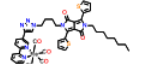
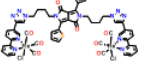
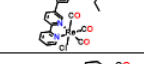
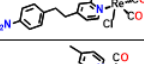
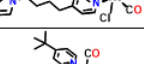
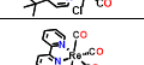
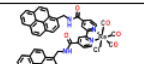
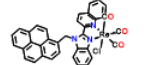
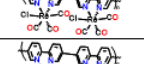
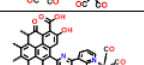
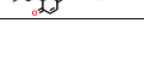
A**B**

Figure S51. SEM-EDX of **2** on CIC on PDPPPTD on carbon paper post electrolysis. (A) SEM image collected at 20 keV with SE2 detector with target area shown. (B) EDX spectrum of target area shown in image

9. Comparison of Supported Lehn-type Catalysts

Table S1. Comparison of state-of-the-art immobilized $\text{Re}(\alpha\text{-diimine})(\text{CO})_3\text{Cl}$ catalysts for electrocatalytic CO_2 -to- CO conversion

Entry #	Catalyst	Support	Anchor Technique	Solvent	E_{onset}	j_{CO} (mA cm^{-2})	TOF_{CO} (hr^{-1})	FE_{CO} (%)	Ref
1		colloid imprinted carbon	non-covalent π - π stacking w/ DPP	Aqueous 0.5 M KHCO_3	-0.75 V vs RHE (1.17 hrs)	0.1	11	49	this work
2		colloid imprinted carbon	non-covalent π - π stacking w/ DPP	Aqueous 0.5 M KHCO_3	-0.75 V vs RHE (1.17 hrs)	0.33	39	53	this work
3		colloid imprinted carbon	direct physisorption	Aqueous 0.5 M KHCO_3	-0.75 V vs RHE (1.17 hrs)	0.05	6	9	this work
4		colloid imprinted carbon	electrochemical oxidative grafting	MeCN 0.1 M TBAPF_6	-2.2 V vs $\text{Fc}^{+/0}$ (2 hrs)	15	468	92 ± 6	7
5		colloid imprinted carbon	pyrrole electropolymerization	Aqueous 0.5 M KHCO_3	-0.66 V vs RHE (6 hrs)	4	52	96 ± 2	1
		MWCNTs	direct physisorption	Aqueous 0.5 M KHCO_3	-0.56 V vs RHE (7 hrs)	4	>5760	99	8
7		carbon cloth	direct physisorption into polymer ion gel	Aqueous 0.1 M KOH + 0.1 M K_2CO_3	-0.68 V vs RHE (24 hrs)	1.19	3.17	50	9
8		Ketjen black	non-covalent π - π stacking w/ pyrene	MeCN 0.1 M TBAPF_6	-2.3 V vs $\text{Fc}^{+/0}$ (1.25 hrs)	not reported	46	70	10
9		edge-plane graphite	non-covalent π - π stacking w/ pyrene	Aqueous 0.5 M KHCO_3	-1.32 V vs NHE (0.5 hrs)	0.34	65000	82 ± 5	11
10		carbon cloth	reductive diazonium electropolymerization	MeCN 0.1 M TBAPF_6	-2.7 V vs $\text{Fc}^{+/0}$ (2 hrs)	11	143640	99	12
11		graphite rods	reductive diazonium electropolymerization	MeCN 0.1 M TBAPF_6	-2.25 V vs $\text{Fc}^{+/0}$ (2 hrs)	10	1800	99	13
12		graphitic carbon	condensation onto quinone edge defects	MeCN 0.1 M TBAPF_6	-2.25 V vs $\text{Fc}^{+/0}$ (1.4 ± 0.3 hrs)	1	9000	96 ± 4	14

10. References

- ¹ Willkomm, J.; Bertin, E.; Atwa, M.; Lin, J. B.; Birss, V.; Piers, W. E., Grafting of a Molecular Rhenium CO₂ Reduction Catalyst onto Colloid-Imprinted Carbon. *ACS Energy Mater. Mat.* **2019**, 2 (4), 2414–2418.
- ² Bharti, S. K.; Raja Roy, R. Quantitative ¹H NMR spectroscopy *Trends Anal. Chem.* **2012**, 35, 5-26.
- ³ Raju, M. V. R.; Lin, H.-C. A Novel Diketopyrrolopyrrole (DPP)-Based [2]Rotaxane for Highly Selective Optical Sensing of Fluoride. *Org. Lett.* **2013**, 15 (6), 1274–1277.
- ⁴ Koenig, J. D. B.; Dubrawski, Z. S.; Rao, K. R.; Willkomm, J.; Gelfand, B. S.; Risko, C.; Piers, W. E.; Welch, G. C. Lowering Electrocatalytic CO₂ Reduction Overpotential Using N-Annulated Perylene Diimide Rhenium Bipyridine Dyads with Variable Tether Length. *J. Am. Chem. Soc.* **2021**, 143, 40, 16849–16864.
- ⁵ Zhanaidarova, A.; Ostericher, A. L.; Miller, C. J.; Jones, S. C.; Kubiak, C. P. Selective Reduction of CO₂ to CO by a Molecular Re(Ethynyl-Bpy)(CO)₃Cl Catalyst and Attachment to Carbon Electrode Surfaces. *Organometallics* **2018**, 38 (6), 1204–1207.
- ⁶ Fulmer, G. R.; Miller, A. J. M.; Sherden, N. H.; Gottlieb, H. E.; Nudelman, A.; Stoltz, B. M.; Bercaw, J. E.; Goldberg, K. I. NMR Chemical Shifts of Trace Impurities: Common Laboratory Solvents, Organics, and Gases in Deuterated Solvents Relevant to the Organometallic Chemist. *Organometallics* **2010**, 29 (9), 2176–2179.
- ⁷ Willkomm, J.; Bertin, E.; Atwa, M.; Lin, J.-B.; Birss, V.; Piers, W. E. Grafting of a Molecular Rhenium CO₂ Reduction Catalyst onto Colloid-Imprinted Carbon *ACS Applied Energy Materials* **2019**, 2, 2414–2418.
- ⁸ Zhanaidarova, A.; Jones, S. C.; Despagnet-Ayoub, E.; Pimentel, B. R.; Kubiak, C. P. Re(^tBu-bpy)(CO)₃Cl Supported on Multi-Walled Carbon Nanotubes Selectively Reduces CO₂ in Water *J. Am. Chem. Soc.* **2019**, 141, 43, 17270–17277.
- ⁹ Sato, S.; McNicholas B. J.; Grubbs, R. H. Aqueous electrocatalytic CO₂ reduction using metal complexes dispersed in polymer ion gels *Chemical Communications* **2020**, 56, 4440–4443.
- ¹⁰ Blakemore, J. D.; Gupta, A.; Warren, J. J.; Brunschwig, B. S.; Gray, H. B. Noncovalent Immobilization of Electrocatalysts on Carbon Electrodes for Fuel Production *J. Am. Chem. Soc.*, **2013**, 135, 18288–18291.
- ¹¹ Sinha, S.; Sonea, A.; Shen, W.; Hanson, S. S.; Warren, J. J. Heterogeneous Aqueous CO₂ Reduction Using a Pyrene-Modified Rhenium(I) Diimine Complex *Inorganic Chemistry* **2019**, 58, 10454–10461.
- ¹² Orchanian, N. M.; Hong, L. E.; Marinescu, S. C. Immobilized Molecular Wires on Carbon-Cloth Electrodes Facilitate CO₂ Electrolysis *ACS Catalysis* **2019**, 9, 9393–9397.
- ¹³ N. M. Orchanian, L. E. Hong, J. A. Skrainka, J. A. Esterhuizen, D. A. Popov and S. C. Marinescu Surface-Immobilized Conjugated Polymers Incorporating Rhenium Bipyridine Motifs for Electrocatalytic and Photocatalytic CO₂ Reduction *ACS Applied Energy Materials* **2019**, 2, 110–123.
- ¹⁴ Oh, S.; Gallagher, J. R.; Miller J. T.; Surendranath, Y. Graphite-Conjugated Rhenium Catalysts for Carbon Dioxide Reduction *J. Am. Chem. Soc.* **2016**, 138, 1820–1823.